

1 **Low** **Syndrome-linked** **endocytic** **adaptors** **direct** **membrane**
2 **cycling** **kinetics** **with** **OCRL** **in** ***Dictyostelium discoideum***.

3 **Running Title:** F&H motifs and OCRL in *Dictyostelium discoideum*

4 **Alexandre Luscher**⁵⁺, **Florian Fröhlich**^{1,7+}, Caroline Barisch⁵, Clare Littlewood⁴, Joe Metcalfe⁴,
5 Florence Leuba⁵, Anita Palma⁶, Michelle Pirruccello^{1,2}, Gianni Cesareni⁶, Massimiliano Stagi⁴, Tobias
6 C. Walther⁷, Thierry Soldati^{5*}, Pietro De Camilli^{1,2,3*}, Laura E. Swan^{1,2,4*}

7 **1.** Department of Cell Biology, Yale University School of Medicine, New Haven, CT 06510, USA

8 **2.** Howard Hughes Medical Institute, Program in Cellular Neuroscience, Neurodegeneration, and
9 Repair, Yale University School of Medicine, New Haven, CT 06510, USA.

10 **3.** Department of Neuroscience and Kavli Institute for Neuroscience, Yale University School of
11 Medicine, New Haven, CT 06510, USA.

12 **4.** Department of Cellular and Molecular Physiology, University of Liverpool, Crown St, Liverpool,
13 L69 3BX, UK

14 **5.** Department of Biochemistry, Faculty of Science, University of Geneva, Science II, 30 quai Ernest-
15 Ansermet, 1211 Geneva-4, Switzerland

16 **6.** Department of Biology, University of Rome, Tor Vergata, Rome Italy

17 **7.** Department of Genetics and Complex Diseases, Harvard School of Public Health, Department of
18 Cell Biology, Harvard Medical School, Howard Hughes Medical Institute, Boston, MA 02115, USA

19 + : contributed equally to this manuscript

20 *: Correspondence : laura.swan@liverpool.ac.uk; pietro.decamilli@yale.edu; Thierry.Soldati@unige.ch

21 Lead correspondence: laura.swan@liverpool.ac.uk

22

1 **Summary** Mutations of the inositol 5-phosphatase OCRL cause Lowe Syndrome (LS), characterized
2 by congenital cataract, low IQ and defective kidney proximal tubule resorption. A key subset of LS
3 mutants abolishes OCRL's interactions with endocytic adaptors containing F&H peptide motifs.
4 Converging unbiased methods examining human peptides and the unicellular phagocytic organism
5 *Dictyostelium discoideum*, reveal that, like OCRL, the *Dictyostelium* OCRL orthologue Dd5P4 binds
6 two proteins closely related to the F&H proteins APPL1 and Ses1/2 (also referred to as IPIP27A/B).
7 In addition, a novel conserved F&H interactor was identified, GxcU (in *Dictyostelium*) and the
8 Cdc42-GEF Frabin (in human cells). Examining these proteins in *Dictyostelium discoideum*, we find
9 that, like OCRL, Dd5P4 acts at well-conserved and physically distinct endocytic stations. Dd5P4
10 functions in coordination with F&H proteins to control membrane deformation at multiple stages of
11 endocytosis, and suppresses GxcU-mediated activity during fluid-phase micropinocytosis. We also
12 reveal that OCRL/Dd5P4 acts at the contractile vacuole, an exocytic osmoregulatory organelle. We
13 propose F&H peptide-containing proteins may be key modifiers of LS phenotypes.

14

15

16 **Keywords:** micropinocytosis, contractile vacuole, Frabin/FGD4, OCRL, Dd5P4, PI(4,5)P₂,
17 PI(3,4,5)P₃, Lowe Syndrome, exocyst, endocytosis,

18

1 **Introduction:**

2 Phosphoinositide lipids (PIPs) are a group of seven phospholipids which, by reversible
3 phosphorylation of the 3', 4' and 5' positions of their cytosolic inositol ring, help specify membrane
4 function and identity. They achieve this chiefly by recruiting cytosolic proteins, such as adaptor
5 proteins for membrane sorting and deformation complexes, allowing co-ordinated recruitment and
6 sorting of transmembrane cargoes in the exo/endocytic cycle. As membranes progress through the
7 exo/endocytic pathways, changes in their PIP "signature" signal a change in their identity, thus
8 modifying membrane function. Humans express at least nine enzymes that act on the 5' position of
9 the lipids PI(4,5)P₂ and/or PI(3,4,5)P₃. Both OCRL (OCRL1) and its paralog INPP5B (also called
10 OCRL2) contain an N-terminal PH domain¹, a central 5'-phosphatase catalytic module, an ASH
11 (ASPM, SPD-2, Hydin) domain² which stabilises a C-terminal catalytically inactive RhoGAP-like
12 domain^{3,4}. The core structure of the OCRL proteins (5' phosphatase and ASH-RhoGAP tandem
13 domain) is exceptionally well conserved during evolution. OCRL-like proteins are found in most
14 eukaryotic lineages, including distantly related eukaryotes such as the protist *Giardia lamblia*⁵,
15 suggesting a significant conserved function.

16 OCRL acts on the 5-phosphates of PI(4,5)P₂ and PI(3,4,5)P₃, two PIPs which are typically enriched at
17 the plasma membrane. However, OCRL is a promiscuous interactor of endocytic proteins, which are
18 found on organelles not typically enriched in these substrate lipids. Endocytic interactors include
19 proteins involved in the initial steps of clathrin-mediated endocytosis^{1,6-8}, early and late endosomal
20 adaptor proteins^{3,4,9,10}, a wide variety of Rab^{11,12} and Rho family GTPases¹³, leading to a distinctive
21 distribution of OCRL-positive intracellular compartments^{3,7,14}.

22 Loss, truncation or missense mutation of OCRL causes the congenital X-linked disorder, oculo-
23 cerebral renal syndrome of Lowe (Lowe Syndrome (LS; OMIM: 309000))¹⁵, affecting the brain, eyes
24 and renal system, or a less severe condition that primarily involves later-onset dysfunction of the renal
25 system, called Dent2 disease (OMIM: 300555)¹⁶. LS and Dent2 disease are caused by a similar
26 spectrum of OCRL¹⁵ mutations, including in one family, the same mutation¹⁷. Missense mutations of

1 the ASH-RhoGAP domain provoke the full spectrum of LS symptoms, namely profound defects in
2 PI(4,5)P₂ metabolism in patient fibroblasts and the clinical triad of kidney, brain and ocular disorders.
3 Previously we have identified that these ASH-RhoGAP mutants are specifically deficient in binding
4 to endocytic proteins containing a helical peptide that we called the F&H motif (for the obligate
5 presence of conserved phenylalanine and histidine residues^{4,10}).

6 The F&H peptide directly binds a surface unique to the OCRL/INPP5B RhoGAP domain. Previous to
7 this study, we had identified F&H motifs in three endocytic proteins, the very early endocytic protein
8 APPL1³, which is a resident of non-canonical PI3P-negative, Rab5-positive endosomes¹⁸ and a pair of
9 later, endosomal adaptors Ses1 and Ses2¹⁰, otherwise known as IPIP27A/B¹⁹, which are resident on
10 canonical PI3P-positive endosomes. Binding of APPL1 and Ses1/2 to OCRL is mutually exclusive
11 and occurs at different endosomal stations defined by the absence or presence of PI3P respectively¹⁰,
12 suggesting formation of OCRL-F&H adaptor protein complexes is subject to regulation by other
13 endocytic factors.

14 The function of F&H motif-dependent interactions of OCRL and INPP5B and their contribution to LS
15 pathology remain elusive. In different systems, fluid-phase endocytosis²⁰ and efficient ciliary traffic²¹
16 require the interaction of OCRL with F&H proteins, suggesting their relevance to LS phenotypes.
17 Ses2/IPIP27B recruits OCRL to sort cation-independent mannose-6-phosphate receptor (Ci-M6PR)²²,
18 a retromer cargo, demonstrating a requirement for OCRL-driven PI(4,5)P₂ dephosphorylation *via*
19 F&H proteins in late endocytic traffic. The F&H binding patch is conserved in most species that
20 express an OCRL-like protein, including a variety of protists and other unicellular eukaryotes
21 including *D. discoideum*, *Trypanosoma brucei*⁴, *Albugo candida* (CCI48278.1, an Oomycete), and
22 *Cyanidioschyzon merolae* (XP_005535444.1, a red alga), suggesting that interactions with F&H
23 peptides are critical to OCRL function. In the above organisms no orthologues of APPL1 and Ses1/2
24 could be identified by primary amino acid sequence similarity or domain structure predictions. We
25 hypothesised that critical functions of OCRL and INPP5B were mediated by yet-unknown F&H
26 peptide-containing binding partners that may have human orthologues, which may help to explain
27 cellular dysfunction in LS.

1 This study aimed to identify ancestral F&H interactors to gain functional insight into the F&H
2 peptide-binding interface of OCRL/INPP5B, and to help understand OCRL dysfunction in LS/Dent2
3 disease. We utilized the unicellular organism *D. discoideum*, where the presence of a single
4 OCRL/INPP5B orthologue (Dd5P4, which has a predicted F&H-motif-binding surface) - avoids
5 complications of vertebrate models that express two, partially redundant, enzymes^{23,24}, OCRL and
6 INPP5B. Importantly, we expected that the study of Dd5P4 would allow us to assess the role of F&H
7 domain binding to OCRL/Dd5P4 in a cellular context where orthologues of APPL1 and Ses1/2 did
8 not appear to be present.

9 Strikingly, our studies showed that not only a network of F&H peptide interactors of OCRL/INPP5B,
10 but also the subcellular localization of these interactors are strongly conserved, suggesting that
11 OCRL-driven hydrolysis of PI(4,5)P₂ or PI(3,4,5)P₃ on endolysosomal organelles is a widely
12 conserved feature of membrane trafficking. We isolated three *D. discoideum* proteins with a *bona fide*
13 F&H motif. Two are related in domain structure to APPL1 and Ses1/2, in spite of divergent amino
14 acid sequence: an APPL1-like early endocytic BAR domain protein and a Ses1/2-like PH domain
15 protein. A third interactor with a novel domain structure is a Rho family GEF, GxcU, orthologous to
16 mammalian Frabin, which we find also has a conserved F&H motif, suggesting its relevance to
17 LS/Dent pathology. We find that overexpression of GxcU leads to endocytic defects which are
18 enhanced by Dd5P4 loss, suggesting Dd5P4 represses GxcU activity. We additionally reveal that both
19 Dd5P4 and the APPL1-like protein are recruited to the contractile vacuole membrane of *D.*
20 *discoideum* upon their kiss-and-run exocytic water discharge, providing new evidence for a role of
21 OCRL-APPL1 partnership in membrane remodelling in the early endocytic pathway.

22 **Results:**

23 **Peptide array experiments confirm F&H motif and identifies Frabin/FGD4 as a potential F&H** 24 **motif containing OCRL interactor**

25 To search for potential new F&H motif-interactors of human OCRL, we first defined the F&H
26 interaction consensus via peptide microarray experiments, to then search for proteins harbouring this

1 consensus in the human proteome (**Figure 1** and **Supplementary Figure 1**). Each residue of the F&H
2 peptide of human Ses1 (13 amino acids) was systematically substituted, and immobilised on
3 nitrocellulose membranes. These membranes were then probed in an overlay assay with a GST fusion
4 of the ASHRhoGAP domain of human OCRL (**Figure 1A**), or of the same domain harbouring a
5 tryptophan to alanine mutation at amino acid 739 (i.e. a tryptophan critically required for F&H motif
6 binding)⁴ to exclude nonspecific interactors. We found that this assay validated the F&H motif
7 deduced by evolutionary conservation of residues in APPL1 and Ses1/2¹⁰ (**Figure 1B,C**). Interaction
8 with OCRL in the overlay assay was absolutely dependent on the presence of F and H residues at
9 positions 2 and 6 of the motif as previously predicted. The peptide array assay, however, appears to
10 favour an APPL1-like mode of binding^{3,4}, which requires only 11aa of the 13aa F&H helical peptide
11 (**Figure 1A,C,D**). The array-derived motif also includes either an R or hydrophobic residue as
12 opposed to the bulky hydrophobic residue at position 9 defined by conservation (**Figure 1B**),
13 generating a slightly less selective F&H motif than that derived by evolutionary conservation.

14 Peptides in the human proteome that fit the peptide-array F&H consensus were synthesised and
15 immobilised on nitrocellulose membranes and probed as above with GST-OCRL-ASHRhoGAP and
16 GST-OCRL-ASHRhoGAP^{W739A} to isolate candidate F&H proteins in humans. Peptides predicted to
17 be inaccessible to cytosolic proteins (i.e. peptides known to be buried in folded domains,
18 transmembrane regions or extracellular domains) were excluded from the analysis. Peptides whose
19 binding to GST-ASHRhoGAP is diminished by at least 50% by W739A mutation (coloured region in
20 **Figure 1D**) were considered to be candidate F&H peptides.

21 This screen identified known F&H peptide interactors Ses1, Ses2, APPL1, as expected, and excluded
22 peptides that we had previously determined using isothermal titration calorimetry (ITC) to be non-
23 specific^{4,10}, (**Supplementary Figure 1**) confirming the specificity of the analysis. It also identified
24 additional potential interactors: PACR, Ace1, Ccdc39, SPG39, WDR81 and Frabin (**Figure 1D**).
25 PACR was excluded on closer inspection as key residues are buried in the plasma membrane²⁵. Ace1,
26 Ccdc39 and SPG39 were also excluded as, based on western blotting on GST-ASHRhoGAP
27 pulldowns in HKC cells (**Supplementary Figure 1**) full-length proteins did not show a specific

1 interaction with the F&H interaction surface of OCRL. WDR81 has a peptide which does not fit in the
2 consensus defined by the conservation of Ses1/2 F&H peptides (**Figure 1B**), but fits with the looser
3 consensus (including an R residue at position 9) defined in **Figure 1C** by peptide array. This low-
4 stringency F&H motif is lost in WDR81 in lower vertebrates such as *Gallus gallus* and *Danio rerio*,
5 suggesting that it is not a conserved interactor of OCRL via this interface.

6 Our final candidate, Frabin/FGD4 is a Cdc42-GEF in the Dbl homology (DH) family of GEFs,
7 consisting of a highly affine actin binding peptide region²⁶, the DH-PH tandem GEF domain followed
8 by two lipid binding domains: the PI3P-binding FYVE domain²⁷ and a second PH domain, which
9 binds a broad spectrum of phosphoinositides including PI(3)P and PI(4,5)P₂²⁷. As we had no antibody
10 that recognised endogenous Frabin, we examined the interaction of Frabin-GFP with endogenous
11 OCRL. Accordingly, a pool of Frabin-GFP was detected along with OCRL on spontaneously
12 generated pinosomes in Cos7 cells (**Figure 1E**). It remained unclear whether this partial
13 colocalization was due to a direct interaction or to the ability of both proteins to independently
14 associate with pinosomes. However, when Cos7 cells expressing Frabin-GFP were subjected to anti-
15 GFP immunoprecipitation, a weak, albeit specific, co-precipitation with OCRL was observed (**Figure**
16 **1F**). Modelling of Frabin using PHYRE2²⁸ to thread the Frabin DH-PH sequence on the known
17 structure of Vav (PDB:3BJI) suggests that the F&H peptide sits on an extended helix of the PH
18 domain (**Figure 1G**), which may be concealed by the neighbouring FYVE domain when Frabin is
19 inactive. The full-length Frabin-OCRL interaction may thus be regulated and only transient, despite
20 the interaction of the Frabin F&H peptide with OCRL being strong.

21 Inspection of databases revealed that the F&H binding patch of OCRL is present in species in which
22 APPL1, Ses1/2, and Frabin orthologues cannot be identified by primary amino acid similarity,
23 suggesting that the original interactor of the OCRL-F&H interface had not yet been identified.
24 Attempts to use unbiased bioinformatics approaches to identify conserved proteins harbouring F&H
25 peptides failed, due largely to the large number of peptides that fit the putative F&H consensus and
26 poor sequence conservation for domains such as PH or BAR domains. Thus, we turned to an ancient

1 unicellular organism, *D. discoideum*, to isolate potential additional evolutionary conserved OCRL
2 F&H interface interactors, and to understand the function of this interface.

3 **Identification of three F&H motif dependent interactors of Dd5P4**

4 The single OCRL-like protein of *D. discoideum*, Dd5P4, has the same overall architecture as
5 mammalian OCRL^{29,30}, except that it lacks the N-terminal PH domain¹, and any identifiable clathrin
6 coat binding motif (**Figure 2A** and **Supplementary Figure 2**). Importantly, the F&H motif binding
7 surface of the RhoGAP-like domain is conserved. Dd5P4 knockout cells (*Dd5P4*⁻ mutants) can be
8 partially rescued by expression of human OCRL²⁹, demonstrating that Dd5P4 and OCRL have well-
9 conserved functions.

10 To identify F&H interactors of Dd5P4 in *D. discoideum*, in *Dd5P4*⁻ cells we expressed GFP fusions
11 of WT Dd5P4 and of a mutant Dd5P4 harbouring a tryptophan to alanine substitution at amino acid
12 position 620, which corresponds to mammalian W739 required for F&H motif binding⁴
13 (**Supplemental Figure 2**). We then analysed triplicate GFP immunoprecipitates from untransfected
14 wild-type cells, alongside GFP-Dd5P4 and GFP-Dd5P4^{W620A} transfected *Dd5P4*⁻knockout cells by
15 mass spectrometry. We found four proteins that were specifically enriched in precipitates from GFP-
16 Dd5P4-expressing cells versus negative control precipitates but not in precipitates from GFP-
17 Dd5P4^{W620A}-expressing cells (**Figure 2B** and for comparison against GFP alone: **Supplementary**
18 **Figure 3**). These four proteins were identified: three uncharacterized gene products, DDB_G0275301,
19 DDB_G0280015, and DDB_G0284853 and the putative Rho-GEF GxcU.

20 To determine if there was a direct F&H peptide mediated interaction with Dd5P4-GFP, we made GST
21 fusions of potential F&H peptides of each protein, performed pulldowns from lysates of *Dd5P4*⁻ cells
22 expressing Dd5P4-GFP, and probed the blot with anti-GFP antibodies. To be certain that we captured
23 any possible interaction, we selected as our test F&H peptide any 13aa stretch in the four proteins that
24 contained the conserved F&H residues, including peptides which did not fit to either of our consensus
25 motifs (**Figure 2C** and **Supplementary Figure 1**). GST-fusions of the F&H peptides of human Ses2
26 and APPL1 were also included. **Figure 2C** shows that Dd5P4-GFP bound the F&H motifs of human

1 APPL1 and Ses2, confirming conservation of the F&H interaction between humans and *D.*
2 *discoideum*. GST fusions of the putative F&H peptides of three of the four candidate *D. discoideum*
3 interactors (DDB_G0275301, DDB_G0280015, and GxcU) bound Dd5P4 – while two low-stringency
4 F&H peptides of protein DDB_G0284853, a mycBP2/Highwire-like protein (Hwr), did not (**Figure**
5 **2C, Supplementary Figure 1C**). We thus conclude that GxcU, DDB_G0275301 (which we called
6 **OCRL-Interacting Bar domain Protein (OIBP)**) and DDB_G0280015 (which we called **PH domain**
7 **Interacting with OCRL (PIO)**) - are *bona fide* direct interactors of the Dd5P4 F&H binding surface.
8 Examining RNA expression profiles³¹, all three F&H-containing proteins are well expressed in cells
9 under non-differentiation conditions, suggesting that all three proteins are available to interact
10 competitively with Dd5P4 at the same time.

11 **The three interactors of Dd5P4 have domain homologies to APPL1, Ses1/2 and Frabin**

12 Remarkably, despite there being no identifiable amino acid sequence homology, modelling²⁸ of the
13 domain structures of the uncharacterized *D. discoideum* F&H motif interactors (OIBP, PIO and
14 GxcU) suggested these to contain signature domains of those of the well-characterized F&H partners
15 of OCRL: APPL1 (a BAR domain) and Ses1/2 (a PH domain with extended PxxP motifs),
16 respectively. GxcU is a DH-PH domain Rho GEF with similar domain structure Frabin which we had
17 identified as a human candidate interactor by peptide array (**Figure 2D**).

18 Using Phyre2²⁸ to model *D. discoideum* sequences onto crystal structures deposited in the PDB
19 database, OIBP (a.a 37-228) displayed a high structural homology with the BAR domain portion of
20 the APPL1 paralogue APPL2 (PDB:4H8S, 98.8% confidence) in spite of a low (12%) sequence
21 identity. The only published study referring to *D. discoideum* OIBP³², reported that this protein was
22 purified in association with macropinosomes, indicating a possible role in
23 endocytosis/macropinocytosis, a function that is conserved with mammalian APPL1/2^{10,18,33}.

24 PIO is a 741aa protein with a predicted PH-domain. Since PIO's PH domain contains a series of long
25 unstructured peptide loops that interfere with accurate tertiary structure prediction, to assess its
26 structural “neighbours” we made structure predictions by searching only the portions of the PH

1 domain of PIO conserved in the closely related species *Dictyostelium purpureum* (XP_003295168.1)
2 (**Supplemental Figure 4**)³⁴. This PH domain falls loosely into the same structural family as the PH
3 domain of PRKD3 (PDB:2D9Z 99.2% confidence 18% sequence similarity) and of PKCD2
4 (PDB:2COA; 99.2% confidence 17% sequence similarity), as does the PH domain of human Ses1
5 (99.9% model confidence, 17% sequence similarity). No function has previously been assigned to this
6 protein.

7 GxcU is one of four *D. discoideum* proteins (GxcU, GxcV, GxcW and GxcX) with a domain structure
8 similar to that of Frabin³⁵: a Dbl-Rho family GEF domain, followed by a PH domain and a FYVE
9 domain. GxcU is largely unstudied, but knockout strains show that this gene is not essential for life³⁶.
10 Frabin (FGD1-related F-actin binding protein) is one of 7 closely related so-called FGD (faciogenital
11 dysplasia) proteins, FGD1-6 and FRG (FGD1-related Cdc42-GEF)/FARP2, thought to function as
12 Cdc42 GEFs. Three FGD proteins are associated with disease: FGD1 is mutated in Aarskog-Scott
13 syndrome³⁷, FGD4/Frabin mutations cause the peripheral neuropathy Charcot Marie Tooth 4H³⁸ and
14 mutations of FGD6 are a risk factor for macular degeneration³⁹. Expanding on our peptide array
15 analysis, we examined all putative F&H motifs in the FGD family regardless of possible presence in
16 folded domains, isolating F&H peptides in Frabin/FGD4, FGD5 (a protein specific to haemopoetic
17 stem cells⁴⁰) and FGD6 (**Figure 2D**).

18 Pulldowns from mouse brain extracts using GST fusions of the putative 13aa F&H motif peptides of
19 each of the three FGD proteins, and of Ses2 and APPL1 as positive controls, revealed that the F&H
20 peptide of Frabin, but not that of FGD5 and FGD6, specifically enriched endogenous OCRL (**Figure**
21 **2E**). The F&H motif captured for Frabin was the same as that independently identified by peptide
22 array (**Figure 1D**).

23 Two unbiased methods, peptide array on human proteins and mass spectrometry in *Dictyostelium*
24 converge on a common set of conserved F&H-peptide harbouring OCRL interactors, APPL1, Ses1/2
25 and Frabin. We hypothesize that distant homologues of at least one of these proteins exist in all cells
26 that express an OCRL protein harbouring this patch.

1 **F&H motif containing proteins are functionally similar in *D. discoideum* and mammals**

2 We next examined the properties of our newly identified F&H binding partners in *D. discoideum*.
3 PIO-GFP fusion proteins were located to compartments of the late-acidic/postlysosomal phase
4 (**Figure 3**). PIO-GFP colocalised with the fluid-phase marker TRITC-dextran (a fluid-phase dye taken
5 up in the phagosomal-lysosomal system and excreted via post-lysosomes) in organelles labelled by 30
6 minutes of fluid phase dye uptake by micropinocytosis, suggesting a function in the endo-lysosomal
7 system. **Figure 3** shows PIO-GFP localization in both WT and *Dd5P4* cells exposed for 30 minutes
8 to TRITC-Dextran. There is very little co-localization between PIO-GFP and dextran label at earlier
9 timepoints (**Figure 3A**, ten minutes dextran pulse) and strong, but not complete colocalization at 30
10 minutes dye uptake (**Figure 3B –D**), suggesting that PIO-GFP labels organelles at the transition
11 between late acidic lysosomes to postlysosomes. This is reminiscent of the localization of Ses1/2
12 proteins at late endosomal stages in mammals^{10,19}.

13 Due to a long low complexity AT-rich stretch in the *D. discoideum* GxcU DNA sequence, it was not
14 possible to clone or to synthesize the *D. discoideum* GxcU cDNA as a GFP fusion. Instead, we
15 synthesized the sequence of the GxcU orthologue from the closely related amoeba *D. intermedium*³⁴,
16 (see **Supplementary Figure 5** for sequence comparison) and expressed it as a fusion protein. Overall,
17 GxcU-GFP appears more punctate in *Dd5P4* cells (**Figures 4A, B**). GxcU-GFP appears on several
18 subcellular structures- including sites of macropinosome formation (**Figure 4C**) and on rare occasions
19 at the plasma membrane some seconds after contractile vacuole (CV) exocytosis events (for a more
20 complete description of CV, please see below) (**Figure 4D**), suggesting that GxcU participates in
21 endocytic events. GxcU-GFP recruitment was evident at the base of the forming macropinocytic cup
22 (**Figure 4C**), which would indicate an early endocytic function, and several seconds after CV fusion
23 (**Figure 4C**) (*i.e.* later than the appearance of OIBP-GFP on these organelles (**Figure 5C**)). A role in
24 coordinating actin-dependent remodelling of the plasma membrane at endocytic sites has also been
25 reported for Frabin^{41,42}. Recruitment of the GxcU-GFP fusion protein appeared delayed in the *Dd5P4*
26 mutant (**Figure 4C**).

1 A C-terminal GFP fusion of OIBP was almost completely cytosolic except for brief and intense
2 ‘flashes’ of recruitment, lasting only a few seconds, near the plasma membrane (**Figure 5A, B** and
3 **Supplementary Movie 4**). As we could see no co-localisation of this signal with TRITC-dextran
4 (*i.e.* the endolysosomal system), we examined another organelle, the contractile vacuole (CV). CVs
5 act to excrete excess fluid to prevent osmotic rupture and are found in many water and soil dwellers.
6 In *D. discoideum*, CVs are a reticulum of bladders and connecting tubules which fill with excess
7 water, undergo rapid kiss-and-run fusion to discharge their contents and locally recycle CV membrane
8 without mixing with the plasma membrane by a striking process of tubulation, fragmentation and
9 reformation of the CV organelle⁴³⁻⁴⁵ (here indicated as ‘collapse phase’). The lipophilic dye FM4-64
10 preferentially incorporates in CV membranes^{46,47}. Co-labelling of the intensely OIBP-GFP-labelled
11 structures with FM4-64 showed that these flashes occurred at the moment at which CVs open to the
12 extracellular medium, during the discharge and collapse phase (**Figure 5A, B**). This observation
13 suggests that OIBP-GFP is recruited as the CV membrane undergoes scission from the plasma
14 membrane and is reformed by tubulation and fragmentation. This localization fits very well with the
15 site of action in mammalian cells of APPL1, a protein with curvature inducer/sensor properties due its
16 BAR domain⁴⁸, which is recruited to endocytic membranes at the earliest stages of endocytosis in
17 mammalian cells¹⁸. When this OIBP-GFP construct was expressed in *Dd5P4* cells, its localization
18 was essentially unchanged (as is the case for its mammalian orthologue APPL1 in OCRL mutant
19 patient fibroblasts¹⁰). However, when we examined the OIBP-GFP ‘flash’ at CV exocytic pores, we
20 found that the lifetime of these events had approximately doubled in *Dd5P4* mutants (**Figure 5B** and
21 **C**).

22 **Novel function of Dd5P4 in contractile vacuole fusion/endocytosis is modulated by F&H peptide** 23 **interactions**

24 Having determined that the F&H proteins of *D. discoideum* recapitulate the localization of their
25 mammalian counterparts, we turned to characterize Dd5P4 recruitment and function on these
26 organelles. Complementation of a *Dd5P4* line with Dd5P4 fused to GFP at either the N- or C-
27 terminus rescued previously-characterized growth deficits³⁴ in these mutants, indicating that the

1 fusion proteins were functional (**Supplementary Figure 5A**). We also successfully rescued the
2 *Dd5P4* growth deficit with the F&H interface mutant GFP-Dd5P4^{W620A}, suggesting that either
3 sufficient overexpression of Dd5P4^{W620A} is enough to overcome any defects in efficient targeting of
4 Dd5P4 activity to membranes, or that, as we had previously observed in human patient fibroblasts⁴,
5 loss of the F&H interface led to loss of OCRL-like activity from very specific membrane
6 subcompartments, and not a generalised deficit in OCRL-mediated traffic.

7 Given the presence of GxcU-GFP and PIO-GFP in the micropinocytic system and the functional
8 requirement for Dd5P4 for micropinocytosis/nutrient uptake (**Supplemental Figure 5A**), we re-
9 examined the subcellular recruitment²⁹ of fluorescently tagged Dd5P4. Despite an established
10 function of Dd5P4 in phagocytosis²⁹, and despite the recruitment of mammalian OCRL to endocytic
11 vesicles engulfing pathogens⁴⁹, neither published studies²⁹ nor our own study with N or C-terminal
12 GFP-tagged Dd5P4 fusions detected a clear accumulation of Dd5P4 on macropinocytic intermediates
13 (labelled by TRITC-dextran in **Supplementary Figure 5B**). We hypothesise that GFP-tagged fusion
14 proteins are likely to be expressed at higher levels than endogenous Dd5P4, and the excess cytosolic
15 fluorescence may mask the presence of a macropinosome-associated pool of the protein.

16 *Dd5P4* cells expressing either GFP-Dd5P4^{WT} or GFP-Dd5P4^{W620A} exhibited marked transient
17 recruitment of GFP fluorescence to organelles that appeared to fuse with the plasma membrane. We
18 excluded post-lysosomes^{50,51} as the organelles in question, as GFP-Dd5P4^{WT} and GFP-Dd5P4^{W620A}
19 fluorescence segregated away from post-lysosomal organelles when cells had been preloaded
20 overnight with TRITC-dextran (**Supplementary Figure 5B**). FM4-64 dye labelling showed both
21 GFP-Dd5P4^{WT} and GFP-Dd5P4^{W620A} were recruited to CVs in the moments before its fusion and
22 collapse at the plasma membrane (**Figure 6D**). We then explored the functional requirement for
23 Dd5P4 and its F&H interface on this organelle.

24 When we imaged FM4-64-labelled cells, we identified frequent CV discharges (see **Figure 6A** for
25 examples of fusion events, showing a full CV, collapse of the organelle and local membrane
26 tubulation). The size of CVs that underwent exocytosis was unchanged between wildtype and *Dd5P4*

1 cells (**Figure 6B**), suggesting that CV biogenesis was grossly normal. Additionally, basal CV fusion,
2 unstimulated by osmotic pressure, occurred at the same rate in both WT and *Dd5P4*⁻ mutant strains.
3 However, 1:1 dilution of the imaging medium with distilled water caused an increase in water
4 pumping and of the CV exocytic rate in WT (**Figure 6C Supplementary Movie 5**), whereas the
5 exocytic rate of CVs did not change from the basal rate in the *Dd5P4*⁻ mutants (**Supplementary**
6 **Movie 6**).

7 Re-expression of GFP-Dd5P4^{WT} in *Dd5P4*⁻ mutants rescued the osmotically-triggered component of
8 CV exocytosis observed in these mutants (**Supplementary Figure 5C**). GFP-Dd5P4^{W620A} showed
9 localization on CVs similar to GFP-Dd5P4^{WT}, speaking against a role of F&H-containing proteins in
10 the recruitment of Dd5P4 to the CV membrane. Comparing the re-expression of GFP-Dd5P4^{WT} in
11 *Dd5P4*⁻ mutants with that of GFP-Dd5P4^{W620A} or the catalytic mutant GFP-Dd5P4^{D319G}, (**Figure 6D**)
12 we noted that the catalytic mutant exerted a dominant effect, almost completely abolishing CV
13 cycling (**Figure 6E**) in both resting and osmotically-stimulated conditions. Additionally, we observed
14 that CV diameter (FM4-64 staining) increased in resting cells expressing GFP-Dd5P4^{D319G} (**Figure**
15 **6D**, quantified in **Figure 6F**). Interestingly, whereas wildtype and W620A Dd5P4 appeared to be
16 recruited to the entire CV membrane at about the time when CV starts decreasing in size due to CV
17 discharge (stars in **Figure 6D**) and persists during the tubulation/collapse phase (arrowheads in
18 **Figure 6D**), GFP-Dd5P4^{D319G} appeared punctate, and did not spread across the CV membrane upon
19 arrival at a FM4-64-labelled organelle. We did not capture any events where GFP-Dd5P4^{D319G} was
20 recruited to a collapsed/tubulating CV. We therefore analysed only the kinetics of GFP recruitment in
21 *Dd5P4*⁻;GFP-Dd5P4^{WT} or *Dd5P4*⁻;GFP-Dd5P4^{W620A} CV fusion events. There was no significant
22 difference in the lifetime of the GFP signal on pre-collapse CVs between the two fusion proteins
23 (**Supplemental Figure 5D**), as in general both fluorescent proteins were recruited when the CV
24 started to discharge and collapse (a few CVs took some time to collapse after GFP-Dd5P4 recruitment
25 as shown in **Supplementary Figure 5D**). We found that GFP-Dd5P4^{W620A} lingered for a significantly
26 longer time than GFP-Dd5P4^{WT} during the process of CV collapse/tubulation (**Figure 6G**) suggesting
27 defects in the process by which membranes tubulate and reform after CVs discharge their content.

1 Taken together, this indicates that catalytic activity is necessary for Dd5P4-mediated CV fusion and
2 that F&H peptide interactions in *D. discoideum* are not essential for recruitment of Dd5P4 to CV
3 membranes, but are necessary for efficient dynamics/remodelling of these membranes during fusion
4 and subsequent re-endocytosis of CV membranes (model in **Figure 6H**).

5 **Dd5P4 loss-of-function deficit in fluid phase dye uptake is phenocopied and enhanced by GxcU**
6 **overexpression.**

7 Loss of Dd5P4 has been shown to cause deficits in fluid-phase micropinocytosis. Neither PIO-GFP
8 nor OIBP-GFP appeared to be recruited to early micropinocytic intermediates, but GxcU-GFP had a
9 wide distribution on organelles including micropinosomes (**Figure 4**), suggesting the two proteins
10 may interact in this process. Overexpression of GxcU-GFP inhibited uptake of TRITC-dextran
11 (**Figure 7A, B**), over all the timescales measured (10minutes, 60 minutes and overnight application of
12 labelled dextran to the culture medium), as observed with Dd5P4⁻ mutants. Both Dd5P4⁻ mutants and
13 GFP-GxcU overexpressors exhibited numerous small dye-positive endolysosomal structures rather
14 than the large lysosomes/postlysosomes found in WT cells, suggestive of a defect in membrane traffic
15 along multiple parts of the endo/lysosomal pathway (see inset images at 60 mins uptake in **Figure**
16 **7A**). GxcU-GFP overexpression in Dd5P4⁻ evoked a profound deficit in dye uptake, suggesting that
17 Dd5P4 activity opposes the action of overexpressed GxcU (**Figure 7B, C**). Cumulatively, this data
18 suggests that OCRL and its F&H protein interactors each act defined points of the membrane cycle as
19 illustrated in **Figure 7D**.

20

21 **Discussion:**

22 Previous studies have shown that interactions of F&H-peptide-containing proteins with
23 OCRL/INPP5B participate in the localization and function of these inositol 5-phosphatases on
24 intracellular membranes^{4,19}. Loss of the F&H-binding surface in mammals very subtly re-localizes
25 OCRL, whereas loss of the OCRL Rab binding interface^{4,52} almost completely delocalizes the protein,
26 suggesting that the F&H interface, as we see in *D. discoideum*, has a specialized function in

1 membrane traffic, rather than a generalized function recruiting OCRL. The F&H motif containing
2 OCRL/INPP5B interactors APPL1 and Ses1/2 (IPIP27A/B), were thought to appear later in evolution
3 than OCRL, as searches of databases had detected APPL1 only in vertebrates³ and Ses/CG12393 in
4 *Drosophila* and other insects, but not in unicellular organisms¹⁰. In contrast, OCRL/INPP5B-like
5 proteins are widely present in unicellular organisms. Amino acids critically required for the F&H
6 interacting surface of OCRL⁴ were highly conserved even in these ancestral OCRL species,
7 suggestive of the presence of yet-to-be-identified F&H interactors in these evolutionary older
8 organisms.

9 We tested this possibility in the social amoeba *D. discoideum*, which expresses a single OCRL
10 orthologue, Dd5P4, displaying an F&H interacting surface. Loss of Dd5P4 is not lethal³⁰, but leads
11 to quantifiable defects in macropinocytosis and growth²⁹, which can be rescued by expression of
12 GFP-fusions of Dd5P4 and of human OCRL, suggesting closely conserved function and subcellular
13 targeting²⁹.

14 To our surprise, we found that the identity of the F&H proteins that interact with OCRL is as well-
15 conserved as the F&H surface itself: in both humans and amoeba, OCRL uses the F&H interface to
16 couple to three proteins, a BAR-domain protein present at the earliest stages of endocytosis (APPL1
17 in humans and OIBP in *D. discoideum*), a PH-domain containing protein on late
18 lysosomes/postlysosomes (Ses1/2 in humans and PIO in *D. discoideum*), and a novel interactor GxcU/
19 Frabin, a Rho family GEF, which in humans is associated with the disorder Charcot Marie Tooth
20 Type 4. Live imaging of GxcU and Frabin showed that both proteins appear at multiple early and later
21 stages of endocytosis. Our data suggests that there is a specific requirement of OCRL phosphatase
22 activity coordinated by different F&H proteins at well-delineated endocytic stations.

23 We also established a novel function for OCRL-like phosphatases in membrane trafficking: in
24 addition to known phenotypes of Dd5P4 loss in *D. discoideum*^{29,30,49,53}, (reduced growth and a defect
25 in both micropinocytosis and phagocytosis), we identified a novel phenotype in axenic cells: Dd5P4
26 controls the rate of fusion and endocytic tubulation/recapture of an osmoregulatory organelle, the

1 contractile vacuole (CV). CV exocytosis is thought to be a “kiss-and-run” process, involving minimal
2 mixing of the CV membrane with the plasma membrane⁵⁴.

3 Notably, we found that Dd5P4 has two separable functions in the CV discharge process: CV fusion,
4 which did not depend on F&H peptide interactions but was blocked by overexpression of a
5 catalytically inactive Dd5P4 fusion protein, and tubulation/reformation (which we indicate as
6 ‘collapse phase’), whose kinetic was influenced by F&H-mediated interactions. We measured
7 extended kinetics of the CV ‘collapse phase’ in GFP-Dd5P4^{W602A} expressing mutants (where the CV
8 fusion rate defects in Dd5P4 knockouts is restored), and the extended kinetics of the OIBP-GFP
9 fusion protein in this same stage in *Dd5P4*.

10 How Dd5P4 interferes with CV fusion is yet unclear, although several functions of OCRL/Dd5P4
11 might be implicated. Disturbances of the actin cytoskeleton cause inappropriate mixing of CV and
12 plasma membranes⁴⁵, leading to CV-resident proton pumps being found at the plasma membrane.
13 Similarly, ‘spillover’ of the transmembrane protein Dajumin, responsible for the biogenesis of CVs, is
14 retrieved from the plasma membrane *via* clathrin/AP2⁵⁵, where mammalian OCRL is also known to
15 act. Thus it is possible that Dd5P4 could have several functions on this organelle, for example
16 regulating underlying actin and/or PI(4,5)P₂ at the CV fusion site, or in trafficking of receptors which
17 are necessary for the CV fusion/reformation cycle. Our images of GFP-Dd5P4^{D419G} show that this
18 mutant protein remains clustered in punctae upon arriving to docked CVs, whereas GFP-Dd5P4^{WT}
19 and GFP-Dd5P4^{W620A} arrive at CVs prior to fusion and then spread over the CV membrane,
20 coincident with the CV starting to fuse and decrease in size. Previous work^{54,56} suggests that during
21 this phase of the CV cycle (docking and fusion-ready) CVs are labelled by Drainin and Rab8 and
22 undergo ‘ring to patch’ transition to allow full fusion. In the absence of the ‘ring to patch’ transition
23 (f.e. in P2XA mutant CVs⁵⁶) CV fusion becomes inefficient, as we have seen in *Dd5P4* mutants. In
24 contrast, the more severe phenotype of GFP-Dd5P4^{D419G} suggests that this mutant may sequester
25 factors such as Rab8^{GTP}. Indeed the swollen CV phenotype found in GFP-Dd5P4^{D419G} is reminiscent
26 of the Rab8^{DN} and *drainin* phenotypes previously published⁵⁴.

1 While there is no direct analogue of this organelle in mammals, the CV is decorated by the small
2 GTPase Rab8 prior to its exocyst-directed fusion with the plasma membrane⁵⁴. Rab8 is a strong
3 interactor of OCRL in mammals^{57,58}, where the interaction is responsible for membrane traffic to the
4 primary cilium²¹. Interestingly, both CV fusion in *D. discoideum*⁵⁴ and growth of cilia involve fusion
5 via the exocyst complex⁵⁹, suggesting OCRL may serve an analogous function in both contexts.

6 The PH domain protein PIO, like its higher-organism counterpart Ses1/2, is a late endocytic protein,
7 only being present on endocytic organelles that are reached by fluid-phase endocytic tracer 30
8 minutes or more after ingestion (**Figure 3**), consistent with a late-endosomal or lysosomal function.
9 The localization of the newly identified OCRL/Dd5P4 interactor, GxcU/Frabin, was particularly
10 intriguing. In human cells, Frabin-GFP has a similar multi-stage recruitment pattern to both early and
11 late endosomal and macropinosocytic membranes^{60,61,62} (**Figure 2, Supplementary Movie 1**). In *D.*
12 *discoideum*, GxcU-GFP was recruited to several distinct stages of the endocytic pathway (**Figures 4E**
13 **and F**), both at what would be considered very early (at the base of the macropinosocytic crown) and at
14 the site of reforming CVs, several seconds after the timepoint when the other F&H interactor, OIBP-
15 GFP appears (*e.g.* **Figure 5A**). While the target of the GxcU GEF activity is not known, the
16 localization of GxcU to macropinosomes is highly reminiscent of the localization of active Rac1^{63,64}.
17 Interestingly, overexpression of GxcU-GFP phenocopied Dd5P4 loss in terms of fluid-phase dye
18 uptake and processing and enhanced the Dd5P4⁻ mutant phenotype (**Figure 7**), suggesting that Dd5P4
19 may be a repressor of GxcU function.

20 In summary, our findings reveal that the network of F&H peptide interactors of OCRL is more
21 evolutionary conserved than expected based on previous studies. Furthermore, in all cases that we
22 examined, selective disruption of the F&H interface of OCRL/Dd5P4 does not significantly impair its
23 localization, but impacts downstream reactions. In *D. discoideum*, F&H mutant Dd5P4 localizes to
24 the same subcompartments as wildtype Dd5P4, but where we made kinetic measurements, we found
25 that lack of F&H interactions affected the kinetics of the trafficking step under study. Likewise F&H-
26 containing interactors of Dd5P4 were recruited to membranes for longer periods in *Dd5P4*⁻ mutants

1 than in wild type, suggesting that co-ordinated activity of OCRL and F&H adaptors is necessary for
2 efficient membrane progression.

3 Our study gives weight to the possibility of functionally relevant amounts of PI(4,5)P₂ being present
4 in the endocytic system under normal conditions. Recent research suggests that PI(4,5)P₂ and/or
5 OCRL catalytic activity has a critical role in membrane traffic separate from its role in at the plasma
6 membrane, including transition from early to late endosomes⁶⁵⁻⁶⁸ and the transition from endosome to
7 trans-Golgi^{8,22}. The presence of conserved, endomembrane-specific interactors for OCRL argues
8 against a function of OCRL solely as a cellular ‘housekeeper’, and suggests instead that OCRL-
9 directed PI(4,5)P₂ on endosomes is assisted and directed by interaction with F&H proteins.

10 Fibroblasts from OCRL- mutated Lowe Syndrome or Dent2 patients are equally deficient in PI(4,5)P₂
11 phosphatase activity⁶⁹, however Dent2 disease fibroblasts manifest milder phenotypes (*e.g.* the
12 degree of defective actin stress fibre formation, abnormal alpha-actinin staining and shortened
13 primary cilia⁶⁹) than their Lowe syndrome counterparts, suggesting the presence of a modifier gene on
14 an autosome. The OCRL paralog INPP5B has been excluded as a phenotype modifier in Lowe/Dent2
15 patients⁶⁹. Given that the F&H interaction is so well conserved and appears to change the kinetics of
16 OCRL-dependant membrane trafficking steps, F&H proteins should be considered as highly likely
17 candidates for modifiers of the Lowe syndrome phenotype.

18 =====

19 ***Acknowledgements:***

20 LES was supported for this project by Wellcome Trust (105616/Z/14/Z), Medical Research Council
21 (MRC/N010035/1) and Lowe Syndrome Association USA. PDC was supported by NIH grants
22 (DA018343; DK082700; NS036251), the Lowe Syndrome Trust, the Lowe Syndrome Association
23 USA and the Kavli Institute for Neuroscience. TS laboratory is supported by multiple grants from the
24 Swiss National Science Foundation. TS is a member of iGE3 (www.ige3.unige.ch). GC was
25 supported by the Italian Association for Cancer Research Grant N (IG 2013 N.14135). MS is
26 supported by North West Cancer Research (CR1081).

1

2 **Author Contributions:** AL, FF, CB, CL, JM,FL, AP, MP, LES performed experiments. AL FF CB

3 FL JM, AP MP MS GC TS, PDC and LES analysed data, FF CB TCW TS PDC and LES contributed

4 to the writing of the manuscript.

5 **Conflict of Interest:** The authors declare no competing financial interests

6

1

2 References:

3

- 4 1 Mao, Y. *et al.* A PH domain within OCRL bridges clathrin-mediated membrane trafficking to
5 phosphoinositide metabolism. *EMBO J* **28**, 1831-1842, doi:10.1038/emboj.2009.155 (2009).
- 6 2 Ponting, C. P. A novel domain suggests a ciliary function for ASPM, a brain size determining
7 gene. *Bioinformatics* **22**, 1031-1035, doi:10.1093/bioinformatics/btl022 (2006).
- 8 3 Erdmann, K. S. *et al.* A role of the Lowe syndrome protein OCRL in early steps of the
9 endocytic pathway. *Dev Cell* **13**, 377-390, doi:10.1016/j.devcel.2007.08.004 (2007).
- 10 4 Pirruccello, M., Swan, L. E., Folta-Stogniew, E. & De Camilli, P. Recognition of the F&H motif
11 by the Lowe syndrome protein OCRL. *Nat Struct Mol Biol* **18**, 789-795,
12 doi:10.1038/nsmb.2071 (2011).
- 13 5 Yichoy, M. *et al.* Lipid metabolism in Giardia: a post-genomic perspective. *Parasitology* **138**,
14 267-278, doi:10.1017/S0031182010001277 (2011).
- 15 6 Taylor, M. J., Perrais, D. & Merrifield, C. J. A high precision survey of the molecular dynamics
16 of mammalian clathrin-mediated endocytosis. *PLoS Biol* **9**, e1000604,
17 doi:10.1371/journal.pbio.1000604 (2011).
- 18 7 Choudhury, R., Noakes, C. J., McKenzie, E., Kox, C. & Lowe, M. Differential clathrin binding
19 and subcellular localization of OCRL1 splice isoforms. *J Biol Chem* **284**, 9965-9973,
20 doi:10.1074/jbc.M807442200 (2009).
- 21 8 Choudhury, R. *et al.* Lowe syndrome protein OCRL1 interacts with clathrin and regulates
22 protein trafficking between endosomes and the trans-Golgi network. *Mol Biol Cell* **16**, 3467-
23 3479, doi:10.1091/mbc.E05-02-0120 (2005).
- 24 9 Nandez, R. *et al.* A role of OCRL in clathrin-coated pit dynamics and uncoating revealed by
25 studies of Lowe syndrome cells. *Elife* **3**, e02975, doi:10.7554/eLife.02975 (2014).
- 26 10 Swan, L. E., Tomasini, L., Pirruccello, M., Lunardi, J. & De Camilli, P. Two closely related
27 endocytic proteins that share a common OCRL-binding motif with APPL1. *Proc Natl Acad Sci*
28 *U S A* **107**, 3511-3516, doi:10.1073/pnas.0914658107 (2010).
- 29 11 Hyvola, N. *et al.* Membrane targeting and activation of the Lowe syndrome protein OCRL1 by
30 rab GTPases. *EMBO J* **25**, 3750-3761, doi:10.1038/sj.emboj.7601274 (2006).
- 31 12 Fukuda, M., Kanno, E., Ishibashi, K. & Itoh, T. Large scale screening for novel rab effectors
32 reveals unexpected broad Rab binding specificity. *Mol Cell Proteomics* **7**, 1031-1042,
33 doi:10.1074/mcp.M700569-MCP200 (2008).
- 34 13 Lichter-Konecki, U., Farber, L. W., Cronin, J. S., Suchy, S. F. & Nussbaum, R. L. The effect of
35 missense mutations in the RhoGAP-homology domain on ocr1 function. *Mol Genet Metab*
36 **89**, 121-128, doi:10.1016/j.ymgme.2006.04.005 (2006).
- 37 14 Williams, C., Choudhury, R., McKenzie, E. & Lowe, M. Targeting of the type II inositol
38 polyphosphate 5-phosphatase INPP5B to the early secretory pathway. *J Cell Sci* **120**, 3941-
39 3951, doi:10.1242/jcs.014423 (2007).
- 40 15 Attree, O. *et al.* The Lowe's oculocerebrorenal syndrome gene encodes a protein highly
41 homologous to inositol polyphosphate-5-phosphatase. *Nature* **358**, 239-242,
42 doi:10.1038/358239a0 (1992).
- 43 16 Hoopes, R. R., Jr. *et al.* Dent Disease with mutations in OCRL1. *Am J Hum Genet* **76**, 260-267,
44 doi:10.1086/427887 (2005).
- 45 17 Hichri, H. *et al.* From Lowe syndrome to Dent disease: correlations between mutations of
46 the OCRL1 gene and clinical and biochemical phenotypes. *Hum Mutat* **32**, 379-388,
47 doi:10.1002/humu.21391 (2011).

- 1 18 Zoncu, R. *et al.* A phosphoinositide switch controls the maturation and signaling properties
2 of APPL endosomes. *Cell* **136**, 1110-1121, doi:10.1016/j.cell.2009.01.032 (2009).
- 3 19 Noakes, C. J., Lee, G. & Lowe, M. The PH domain proteins IPIP27A and B link OCRL1 to
4 receptor recycling in the endocytic pathway. *Mol Biol Cell* **22**, 606-623,
5 doi:10.1091/mbc.E10-08-0730 (2011).
- 6 20 Oltrabella, F. *et al.* The Lowe syndrome protein OCRL1 is required for endocytosis in the
7 zebrafish pronephric tubule. *PLoS Genet* **11**, e1005058, doi:10.1371/journal.pgen.1005058
8 (2015).
- 9 21 Coon, B. G. *et al.* The Lowe syndrome protein OCRL1 is involved in primary cilia assembly.
10 *Hum Mol Genet* **21**, 1835-1847, doi:10.1093/hmg/ddr615 (2012).
- 11 22 Billcliff, P. G. *et al.* OCRL1 engages with the F-BAR protein pacsin 2 to promote biogenesis of
12 membrane-trafficking intermediates. *Mol Biol Cell* **27**, 90-107, doi:10.1091/mbc.E15-06-0329
13 (2016).
- 14 23 Bernard, D. J. & Nussbaum, R. L. X-inactivation analysis of embryonic lethality in *Ocrl* wt^{-/-};
15 *Inpp5b*^{-/-} mice. *Mamm Genome* **21**, 186-194, doi:10.1007/s00335-010-9255-9 (2010).
- 16 24 Janne, P. A. *et al.* Functional overlap between murine *Inpp5b* and *Ocrl1* may explain why
17 deficiency of the murine ortholog for OCRL1 does not cause Lowe syndrome in mice. *J Clin*
18 *Invest* **101**, 2042-2053, doi:10.1172/JCI2414 (1998).
- 19 25 McCulloch, D. A. *et al.* ADP-ribosylation factor-dependent phospholipase D activation by
20 VPAC receptors and a PAC(1) receptor splice variant. *Mol Pharmacol* **59**, 1523-1532 (2001).
- 21 26 Banerjee, J., Fischer, C. C. & Wedegaertner, P. B. The amino acid motif L/IxxFE defines a
22 novel actin-binding sequence in PDZ-RhoGEF. *Biochemistry* **48**, 8032-8043,
23 doi:10.1021/bi9010013 (2009).
- 24 27 Catimel, B. *et al.* The PI(3)P interactome from a colon cancer cell. *J Proteomics* **82**, 35-51,
25 doi:10.1016/j.jprot.2013.01.031 (2013).
- 26 28 Kelley, L. A., Mezulis, S., Yates, C. M., Wass, M. N. & Sternberg, M. J. The Phyre2 web portal
27 for protein modeling, prediction and analysis. *Nat Protoc* **10**, 845-858,
28 doi:10.1038/nprot.2015.053 (2015).
- 29 29 Loovers, H. M. *et al.* Regulation of phagocytosis in *Dictyostelium* by the inositol 5-
30 phosphatase OCRL homolog Dd5P4. *Traffic* **8**, 618-628, doi:10.1111/j.1600-
31 0854.2007.00546.x (2007).
- 32 30 Loovers, H. M. *et al.* A diverse family of inositol 5-phosphatases playing a role in growth and
33 development in *Dictyostelium discoideum*. *J Biol Chem* **278**, 5652-5658,
34 doi:10.1074/jbc.M208396200 (2003).
- 35 31 Van Driessche, N. *et al.* A transcriptional profile of multicellular development in
36 *Dictyostelium discoideum*. *Development* **129**, 1543-1552 (2002).
- 37 32 Journet, A. *et al.* Investigating the macropinocytic proteome of *Dictyostelium amoebae* by
38 high-resolution mass spectrometry. *Proteomics* **12**, 241-245, doi:10.1002/pmic.201100313
39 (2012).
- 40 33 Bohdanowicz, M., Balkin, D. M., De Camilli, P. & Grinstein, S. Recruitment of OCRL and
41 *Inpp5B* to phagosomes by Rab5 and APPL1 depletes phosphoinositides and attenuates Akt
42 signaling. *Mol Biol Cell* **23**, 176-187, doi:10.1091/mbc.E11-06-0489 (2012).
- 43 34 Schaap, P. *et al.* Molecular phylogeny and evolution of morphology in the social amoebas.
44 *Science* **314**, 661-663, doi:10.1126/science.1130670 (2006).
- 45 35 Vlahou, G. & Rivero, F. Rho GTPase signaling in *Dictyostelium discoideum*: insights from the
46 genome. *Eur J Cell Biol* **85**, 947-959, doi:10.1016/j.ejcb.2006.04.011 (2006).
- 47 36 Wang, Y., Senoo, H., Sesaki, H. & Iijima, M. Rho GTPases orient directional sensing in
48 chemotaxis. *Proc Natl Acad Sci U S A* **110**, E4723-4732, doi:10.1073/pnas.1312540110
49 (2013).

- 1 37 Pasteris, N. G. *et al.* Isolation and characterization of the faciogenital dysplasia (Aarskog-
2 Scott syndrome) gene: a putative Rho/Rac guanine nucleotide exchange factor. *Cell* **79**, 669-
3 678 (1994).
- 4 38 Delague, V. *et al.* Mutations in FGD4 encoding the Rho GDP/GTP exchange factor FRABIN
5 cause autosomal recessive Charcot-Marie-Tooth type 4H. *Am J Hum Genet* **81**, 1-16,
6 doi:10.1086/518428 (2007).
- 7 39 Huang, L. *et al.* A missense variant in FGD6 confers increased risk of polypoidal choroidal
8 vasculopathy. *Nat Genet* **48**, 640-647, doi:10.1038/ng.3546 (2016).
- 9 40 Gazit, R. *et al.* Fgd5 identifies hematopoietic stem cells in the murine bone marrow. *J Exp*
10 *Med* **211**, 1315-1331, doi:10.1084/jem.20130428 (2014).
- 11 41 Horn, M. *et al.* Myelin is dependent on the Charcot-Marie-Tooth Type 4H disease culprit
12 protein FRABIN/FGD4 in Schwann cells. *Brain* **135**, 3567-3583, doi:10.1093/brain/aws275
13 (2012).
- 14 42 Nakanishi, H. & Takai, Y. Frabin and other related Cdc42-specific guanine nucleotide
15 exchange factors couple the actin cytoskeleton with the plasma membrane. *J Cell Mol Med*
16 **12**, 1169-1176, doi:10.1111/j.1582-4934.2008.00345.x (2008).
- 17 43 Gerisch, G., Heuser, J. & Clarke, M. Tubular-vesicular transformation in the contractile
18 vacuole system of Dictyostelium. *Cell Biol Int* **26**, 845-852 (2002).
- 19 44 Clarke, M. *et al.* Dynamics of the vacuolar H(+)-ATPase in the contractile vacuole complex
20 and the endosomal pathway of Dictyostelium cells. *J Cell Sci* **115**, 2893-2905 (2002).
- 21 45 Heuser, J. Evidence for recycling of contractile vacuole membrane during osmoregulation in
22 Dictyostelium amoebae--a tribute to Gunther Gerisch. *Eur J Cell Biol* **85**, 859-871,
23 doi:10.1016/j.ejcb.2006.05.011 (2006).
- 24 46 Nishihara, E., Shimmen, T. & Sonobe, S. New aspects of membrane dynamics of Amoeba
25 proteus contractile vacuole revealed by vital staining with FM 4-64. *Protoplasma* **231**, 25-30,
26 doi:10.1007/s00709-007-0247-x (2007).
- 27 47 Heuser, J., Zhu, Q. & Clarke, M. Proton pumps populate the contractile vacuoles of
28 Dictyostelium amoebae. *J Cell Biol* **121**, 1311-1327 (1993).
- 29 48 McMahon, H. T. & Boucrot, E. Membrane curvature at a glance. *J Cell Sci* **128**, 1065-1070,
30 doi:10.1242/jcs.114454 (2015).
- 31 49 Weber, S. S., Ragaz, C. & Hilbi, H. The inositol polyphosphate 5-phosphatase OCRL1 restricts
32 intracellular growth of Legionella, localizes to the replicative vacuole and binds to the
33 bacterial effector LpnE. *Cell Microbiol* **11**, 442-460, doi:10.1111/j.1462-5822.2008.01266.x
34 (2009).
- 35 50 King, J. S. *et al.* WASH is required for lysosomal recycling and efficient autophagic and
36 phagocytic digestion. *Mol Biol Cell* **24**, 2714-2726, doi:10.1091/mbc.E13-02-0092 (2013).
- 37 51 Gopaldass, N. *et al.* Dynamin A, Myosin IB and Abp1 couple phagosome maturation to F-
38 actin binding. *Traffic* **13**, 120-130, doi:10.1111/j.1600-0854.2011.01296.x (2012).
- 39 52 Luo, N. *et al.* OCRL localizes to the primary cilium: a new role for cilia in Lowe syndrome.
40 *Hum Mol Genet* **21**, 3333-3344, doi:10.1093/hmg/dds163 (2012).
- 41 53 Hilbi, H., Weber, S. & Finsel, I. Anchors for effectors: subversion of phosphoinositide lipids by
42 legionella. *Front Microbiol* **2**, 91, doi:10.3389/fmicb.2011.00091 (2011).
- 43 54 Essid, M., Gopaldass, N., Yoshida, K., Merrifield, C. & Soldati, T. Rab8a regulates the exocyst-
44 mediated kiss-and-run discharge of the Dictyostelium contractile vacuole. *Mol Biol Cell* **23**,
45 1267-1282, doi:10.1091/mbc.E11-06-0576 (2012).
- 46 55 Macro, L., Jaiswal, J. K. & Simon, S. M. Dynamics of clathrin-mediated endocytosis and its
47 requirement for organelle biogenesis in Dictyostelium. *J Cell Sci* **125**, 5721-5732,
48 doi:10.1242/jcs.108837 (2012).
- 49 56 Parkinson, K. *et al.* Calcium-dependent regulation of Rab activation and vesicle fusion by an
50 intracellular P2X ion channel. *Nat Cell Biol* **16**, 87-98, doi:10.1038/ncb2887 (2014).

- 1 57 Hagemann, N., Hou, X., Goody, R. S., Itzen, A. & Erdmann, K. S. Crystal structure of the Rab
2 binding domain of OCRL1 in complex with Rab8 and functional implications of the
3 OCRL1/Rab8 module for Lowe syndrome. *Small GTPases* **3**, 107-110, doi:10.4161/sgtp.19380
4 (2012).
- 5 58 Hou, X. *et al.* A structural basis for Lowe syndrome caused by mutations in the Rab-binding
6 domain of OCRL1. *EMBO J* **30**, 1659-1670, doi:10.1038/emboj.2011.60 (2011).
- 7 59 Mukherjee, D., Sen, A. & Aguilar, R. C. RhoGTPase-binding proteins, the exocyst complex and
8 polarized vesicle trafficking. *Small GTPases* **5**, e28453, doi:10.4161/sgtp.28453 (2014).
- 9 60 Hayakawa, A. *et al.* Structural basis for endosomal targeting by FYVE domains. *J Biol Chem*
10 **279**, 5958-5966, doi:10.1074/jbc.M310503200 (2004).
- 11 61 Kim, Y. *et al.* Association of frabin with specific actin and membrane structures. *Genes Cells*
12 **7**, 413-420 (2002).
- 13 62 Brooks, A. B. *et al.* MYO6 is targeted by Salmonella virulence effectors to trigger PI3-kinase
14 signaling and pathogen invasion into host cells. *Proc Natl Acad Sci U S A* **114**, 3915-3920,
15 doi:10.1073/pnas.1616418114 (2017).
- 16 63 Rivero, F. & Xiong, H. Rho Signaling in Dictyostelium discoideum. *Int Rev Cell Mol Biol* **322**,
17 61-181, doi:10.1016/bs.ircmb.2015.10.004 (2016).
- 18 64 Marinovic, M., Sostar, M., Filic, V., Antolovic, V. & Weber, I. Quantitative imaging of Rac1
19 activity in Dictyostelium cells with a fluorescently labelled GTPase-binding domain from
20 DPAKa kinase. *Histochem Cell Biol* **146**, 267-279, doi:10.1007/s00418-016-1440-9 (2016).
- 21 65 Muriel, O., Tomas, A., Scott, C. C. & Gruenberg, J. Moesin and cortactin control actin-
22 dependent multivesicular endosome biogenesis. *Mol Biol Cell* **27**, 3305-3316,
23 doi:10.1091/mbc.E15-12-0853 (2016).
- 24 66 Vicinanza, M. *et al.* OCRL controls trafficking through early endosomes via PtdIns4,5P(2)-
25 dependent regulation of endosomal actin. *EMBO J* **30**, 4970-4985,
26 doi:10.1038/emboj.2011.354 (2011).
- 27 67 Henmi, Y. *et al.* PtdIns4KIIalpha generates endosomal PtdIns(4)P and is required for receptor
28 sorting at early endosomes. *Mol Biol Cell* **27**, 990-1001, doi:10.1091/mbc.E15-08-0564
29 (2016).
- 30 68 Sun, Y., Hedman, A. C., Tan, X., Schill, N. J. & Anderson, R. A. Endosomal type Igamma PIP 5-
31 kinase controls EGF receptor lysosomal sorting. *Dev Cell* **25**, 144-155,
32 doi:10.1016/j.devcel.2013.03.010 (2013).
- 33 69 Montjean, R. *et al.* OCRL-mutated fibroblasts from patients with Dent-2 disease exhibit
34 INPP5B-independent phenotypic variability relatively to Lowe syndrome cells. *Hum Mol*
35 *Genet* **24**, 994-1006, doi:10.1093/hmg/ddu514 (2015).

36

37

1 **Figure legends:**

2 **Figure 1:** Overlay assay detects new F&H candidate proteins. **A)** Peptide overlay experiments
3 confirm the established consensus sequence for F&H peptides. Each residue was systematically
4 substituted in the Ses1 F&H peptide (*vertical*: the original residue in the peptide, *horizontal*:
5 substituted residue) immobilised on nitrocellulose and probed with GST-hOCRL-ASHRhoGAP or the
6 non-F&H binding GST-hOCRL-ASHRhoGAP^{W739A} to control for non-specific binding. **B)** F&H
7 consensus derived from sequence conservation of F&H peptides in Ses1/2 proteins. **C)** F&H
8 consensus derived from peptide overlay. **D)** Naturally occurring human peptides which fall within the
9 F&H consensus derived in **C** were immobilised on nitrocellulose and probed with wild-type GST-
10 hOCRL-ASHRhoGAP (**Figure 1D**, *x-axis*) and control as before. WT binding intensity is plotted
11 against the difference (*y-axis*, arbitrary units) in intensity of binding to WT and W739A control. We
12 defined candidate interactors as peptides in the upper left quadrant of the graph (*i.e* peptides whose
13 binding to GST-hOCRL-ASHRhoGAP is reduced by over 50% by the W739A mutation). All known
14 F&H peptide interactors (red) were isolated by this analysis, including two identical Ses1 peptides.
15 Peptides determined as non-interactors by isothermal titration calorimetry are excluded (yellow)
16 (**Supplementary Figure 1B**). The Frabin F&H peptide (green) was isolated as an interactor in this
17 assay. **E)** Ruby-OCRL and Frabin-GFP are found together on pinosomal compartments in Cos7, see
18 **Supplementary Movie 1**. Scale bar: 3µm. **F)** Full length Frabin-GFP immunoprecipitations isolated
19 a weak but specific interaction with endogenous OCRL in Cos7 cells. **G)** predicted structure of the
20 Frabin DH-PH module shows the Frabin F&H peptide (red) is found on an extended alpha helix of the
21 Frabin PH1 domain.

22

1

2 **Figure 2:** The F&H interface specifically interacts with three proteins in *D. discoideum*. **A)**
3 Comparison of human INPP5B/OCRL and Dd5P4 amino acid sequences. **B)** Analysis of *Dd5P4*;
4 GFP-Dd5P4^{WT} vs *Dd5P4*; GFP-Dd5P4^{W620A} immunoprecipitates shows enrichment of four possible
5 interactors of the F&H surface of Dd5P4. Points labelled in Black are proteins that were also enriched
6 in an analysis of wild-type vs *Dd5P4*; GFP-Dd5P4^{WT} (**Supplementary Figure 3**). **C)** all possible
7 F&H peptides in the four putative F&H-surface interactors were produced as GST fusions and
8 purified on beads. These beads were exposed to lysates of *D. discoideum* expressing GFP-Dd5P4^{WT}.
9 **D)** Domain structure of F&H interactors in *D. discoideum* and humans, with validated interacting
10 peptides shown below. *DH*: Dbl Homology domain, *PH*: Phox Homology homain, *F*: FYVE domain,
11 *BAR*: Bin-Amphiphysin-Rvs domain, *PTB*: phosphotyrosine binding domain. The location of
12 validated F&H peptide consensus is highlighted in red, unsuccessful F&H motifs are highlighted in
13 yellow **E)** GST and GST-F&H peptides were exposed to HKC cell lysate. A specific interaction with
14 endogenous OCRL was found with the known interactors Ses2 and APPL1.

15

16 **Figure 3:** PIO-GFP labels a late lysosomal station. **A)** In WT cells PIO-GFP (*arrows*) does not
17 colocalise with early lysosomal intermediates labelled by 10 minutes of fluid-phase dextran uptake
18 (*arrowheads*) **B)** at 30 minutes, fluid phase dextran (*red*) marks some, but not all PIO-GFP positive
19 compartments. **C,D)** There is no significant change in PIO-GFP localisation in *Dd5P4*⁻ cells: two
20 examples of PIO-GFP expressing *Dd5P4*⁻ cells (one cytosolic, one punctate) labelled for 30 minutes
21 with TRITC-dextran. Scale bar: 5µm.

22

23 **Figure 4:** GxcU-GFP labels several endocytic intermediates. Wide-field microscopy (left panel) and
24 confocal microscopy (right panel) of GxcU-GFP expressing cells **A)** wildtype cells expressing GFP-
25 GxcU. **B)** GxcU-GFP is more punctate in *Dd5P4*⁻ cells. Scale bars in B: 10 µm. **C)** GxcU-GFP can be
26 detected on phagosomes in both WT (upper) and *Dd5P4*⁻ (lower) cells. Gallery of images 0.25Hz (see

1 **Supplementary Movies 2 and 3 D)** GxcU-GFP is also (rarely) detectible several seconds after CV
2 collapse (site of CV collapse marked by red arrows) in both WT and *Dd5P4*⁻ cells, gallery at 1Hz.

3

4 **Figure 5:** F&H interactions contribute to membrane reformation kinetics at the contractile vacuole.
5 OIBP-GFP in **A)** wildtype cells. Expression of OIBP-GFP is largely cytosolic except for endocytic
6 structures associated with contractile vacuoles, labelled in by FM4-64 (red). Shown is a gallery of
7 images showing CV fusing *en face*, image rate 0.25Hz *Yellow Star:* CV beginning to collapse. (See
8 **Supplementary Movie 4).** **B)** Gallery showing OIBP-GFP recruitment to osmotically-triggered CV
9 fusion events imaged at 1Hz *upper panel:* WT cells. *Lower panel:* *Dd5P4*⁻ cells. Scale Bars in A and
10 B: 4µm. **C)** Lifetime of OIBP-GFP fluorescence during CV collapse (start of the collapse indicated by
11 yellow star) is approximately twice as long in *Dd5P4*⁻ cells. N=21 WT events, N=43 *Dd5P4*⁻ events,
12 two sided student's *T*-test: P<0.0005.

13

14 **Figure 6:** CV dynamics in *Dd5P4* mutants and rescues **A)** FM4-64 dye labelling of CV membranes in
15 WT and *Dd5P4*⁻ cells show CV distribution is similar. Lower panel: CV collapse event (frames from
16 0.25 Hz movie), quantified in **6C** and **E**. *Star* indicates a CV about to collapse, *arrow* indicates the
17 collapsed CV membrane. **Scale bar:** 2µm **B).** Size at widest point of CVs undergoing fusion is
18 unchanged by *Dd5P4* loss: N=179 (WT), =87 (*Dd5P4*⁻). **C).** rate of CV fusion triggered by 1:1
19 osmotic stimulus is strongly reduced, but not abolished, in *Dd5P4*⁻ mutants. Average of 3 movies per
20 condition, StdDev, two-sided student's *T*-test.**D)** Recruitment of GFP-*Dd5P4* constructs to contractile
21 vacuoles marked by FM4-64. GFP-*Dd5P4*^{WT} and GFP-*Dd5P4*^{W620A} are recruited to CVs at the
22 moment that the CV starts to collapse (marked by a *red star*) and persists at the moment of full
23 collapse (*arrow*). GFP-*Dd5P4*^{D319G} is recruited in punctae to the CV but do not appear to spread over
24 the CV surface, CVs appear enlarged. Movie: 0.25Hz. **Scale bars:** 2µm. **E)** FM4-46 labelling shows
25 that *Dd5P4*⁻; GFP-*Dd5P4*^{D319G} cells exhibit significantly reduced CV fusion/collapse in both basal and
26 osmotically stimulated conditions. *Dd5P4*⁻; GFP-*Dd5P4*^{W620A} cells show a similar rate of CV fusions

1 as *Dd5P4*⁻; GFP-Dd5P4^{WT}. number of movies per condition indicated on graph. Student *T*-Test. See
2 **Supplementary Movies 7 and 8** for live imaging of GFP signal. **F)** Cells in basal conditions show
3 significantly larger CV diameters in *Dd5P4*⁻; GFP-Dd5P4^{D319G} cells. **G)** GFP signal in collapse phase
4 lasts longer in *Dd5P4*⁻; GFP-Dd5P4^{W620A} cells than in cells re-expressing GFP-Dd5P4^{WT}. **H)** Model of
5 Dd5P4 action during CV cycle

6

7

8

9

10

11 **Figure 7:** GxcU-GFP overexpression and Dd5P4 loss show similar effects in micropinocytic dye
12 uptake and subsequent membrane trafficking. **A)** timed application of TRITC-dextran (red) shows
13 defects in initial micropinocytic uptake (10 minutes) and subsequent membrane trafficking (60
14 minutes) in both *Dd5P4*⁻ cells and GxcU-GFP overexpressors, which is enhanced by GxcU-GFP
15 overexpression in the *Dd5P4*⁻ background. Individual cells are shown *inset*. **B)** Deficits in dye uptake
16 are not resolved by longer exposure to dye (overnight labelling). TRITC-dextran label is shown in
17 false colour scale for ease of comparison. Scale Bars in **A, B:** 8µm. **C)** GFP-GxcU overexpression
18 enhances dye uptake defects caused by Dd5P4 loss. Fluorescence per cell after overnight TRITC-
19 dextran uptake, ANOVA. **D)** localisation of Dd5P4 and F&H-motif-containing interactors

20

21 **Supplementary Figure 1, related to Figure 1.** Determination of candidate F&H proteins in humans
22 by peptide array. **A)** Western Blot on three candidate proteins in HKC lysates showed no specific
23 interaction with the OCRL F&H interface. **B)** ITC reveals the putative F&H peptide of Dynein heavy
24 chain to be a non-specific interactor. **C)** Summary of tested human F&H peptides. Proteins labelled in

1 red have been validated in previous publications. Proteins in yellow have been confirmed to be non-
2 interactors of the OCRL-F&H motif by Isothermal Titration Calorimetry. Red residues are common to
3 Ses1/2 and APPL1, blue residues are conserved in Ses proteins. Purple residues are at key positions
4 and fall outside the Ses/APPL1 consensus. (MS= mass spectrometry on GFP-OCRL precipitates), WB
5 (Western Blot) ITC (Isothermal titration calorimetry). + published in Swan et al PNAS 2010 and
6 Pirruccello et al NSMB 2011; * Nandez et al eLIFE 2014.

7

8 **Supplementary Figure 2, related to Figure 2.** Sequence conservation between Dd5P4 and
9 human INPP5B and OCRL. Domains are indicated by lines under the sequence alignment.
10 *Identical residues* are shaded. *Boxed residues*: interaction motifs for clathrin and AP2 (unique to
11 OCRL). *Dot*: catalytic residue. *Arrowhead*: key Rab binding residue. *Starred residues*:
12 mediate contact with F&H peptides. *Residues marked in red*: mutated in this study.

13

14 **Supplementary Figure 3, related to Figure 2:** Analysis of peptide enrichment of GFP
15 immunoprecipitates from **A**) WT vs *Dd5P4*;GFP-Dd5P4^{WT} and **B**) WT vs *Dd5P4*;GFP-Dd5P4^{W620A}
16 shows that putative F&H proteins (**Figure 2B**) are specifically enriched in precipitates from GFP-
17 Dd5P4^{WT} expressing cells.

18

19 **Supplementary Figure 4:** related to **Figures 3 and 4.** Sequences of PIO and GxcU proteins **A**) The
20 predicted PH domains of *D discoideum* PIO (aa 543-741) and *D. purpureum* PIO partial sequence (aa
21 200-401). Identical residues are shaded. *Boxed region* was used to search crystal structures with
22 Phyre2 **B**) Conservation of amino acid sequence between *D discoideum* and *D intermedium* GxcU
23 genes. The Rho-GEF, PH and FYVE domains are strongly conserved, as is the F&H peptide sequence
24 (boxed residues).

1

2 **Supplementary Figure 5, related to Figure 6:** GFP-Dd5P4^{W620A} rescues many aspects of *Dd5P4*
3 dysfunction. **A)** N-terminal and C-terminal GFP fusions of Dd5P4, and an N-terminal GFP labelled
4 mutant of the F&H surface (W620A) all restore growth in a *Dd5P4* background. N=3 independent
5 growth curves per genotype. **B)** Both GFP-Dd5P4 and GFP-Dd5P4^{W620A} are largely cytosolic (as seen
6 in previous publications), but GFP fluorescence is found on cytosolic organelles which are not part of
7 the endocytic system (negative for 7KDa Dextran label). Arrowheads show GFP accumulation at
8 collapsing contractile vacuole. **C)** Re-expression of GFP-tagged Dd5P4 restores osmotically-triggered
9 CV fusion in cells labelled with FM4-64, N=3 independent movies per genotype, normalised to
10 corresponding wildtype value. **D)** Lifetime of GFP-labelled CVs imaged at 0.2Hz *prior* to fusion in
11 *Dd5P4*; GFP-Dd5P4^{WT} cells is not significantly different to that of *Dd5P4*; GFP-Dd5P4^{W620A}
12 expressers: n= 28 GFP-Dd5P4^{WT} labelled events, n=67 GFP-Dd5P4^{W620A} labelled events, Student's t-
13 test. All CV exocytosis events which were GFP positive either in the pre-collapse or collapse phase
14 were analysed. The majority of GFP-Dd5P4^{WT} CVs are positive for GFP only in the collapse phase
15 (i.e are recorded as zero frames before CV collapse).

16

17 **Table 1:** constructs and *Dictyostelium* cell lines used in this manuscript

18 **Supplementary Movie 1, related to Figure 1:** Ruby-OCRL (red) and Frabin-GFP (green) are found
19 together on pinosomal compartments in Cos7. Images 0.25Hz. Scale Bar 3µm.

20 **Supplementary Movie 2, related to Figure 4:** GxcU-GFP can be detected on phagosomes
21 in WT cells. Images 0.25Hz. Scale Bar 15µm.

22 **Supplementary Movie 3, related to Figure 4:** GxcU-GFP can be detected on phagosomes
23 in *Dd5P4* cells. Images 0.25Hz. Scale Bar 15µm.

- 1 **Supplementary Movie 4, related to Figure 5:** Recruitment of a C-terminal GFP fusion of OIBP
- 2 (green). Contractile vacuoles are labelled by FM4-64 (red). Images 0.25Hz. Scale Bar 10 μ m.

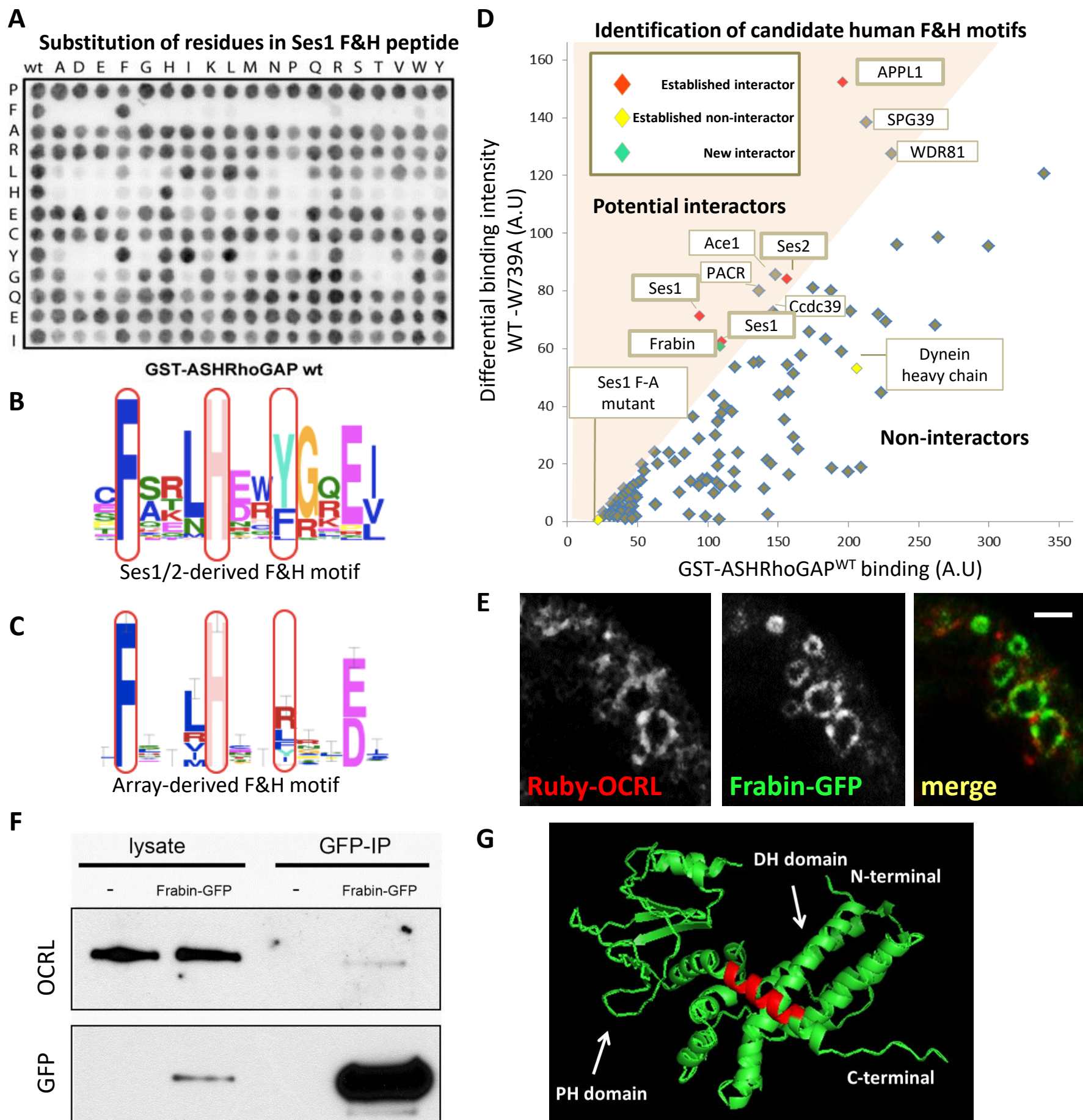
- 3 **Supplementary Movie 5, related to Figure 6:** 1:1 dilution-of imaging medium with distilled water
- 4 caused an increase CV exocytosis rate in WT. Images 0.2 Hz. Scale Bar 15 μ m.

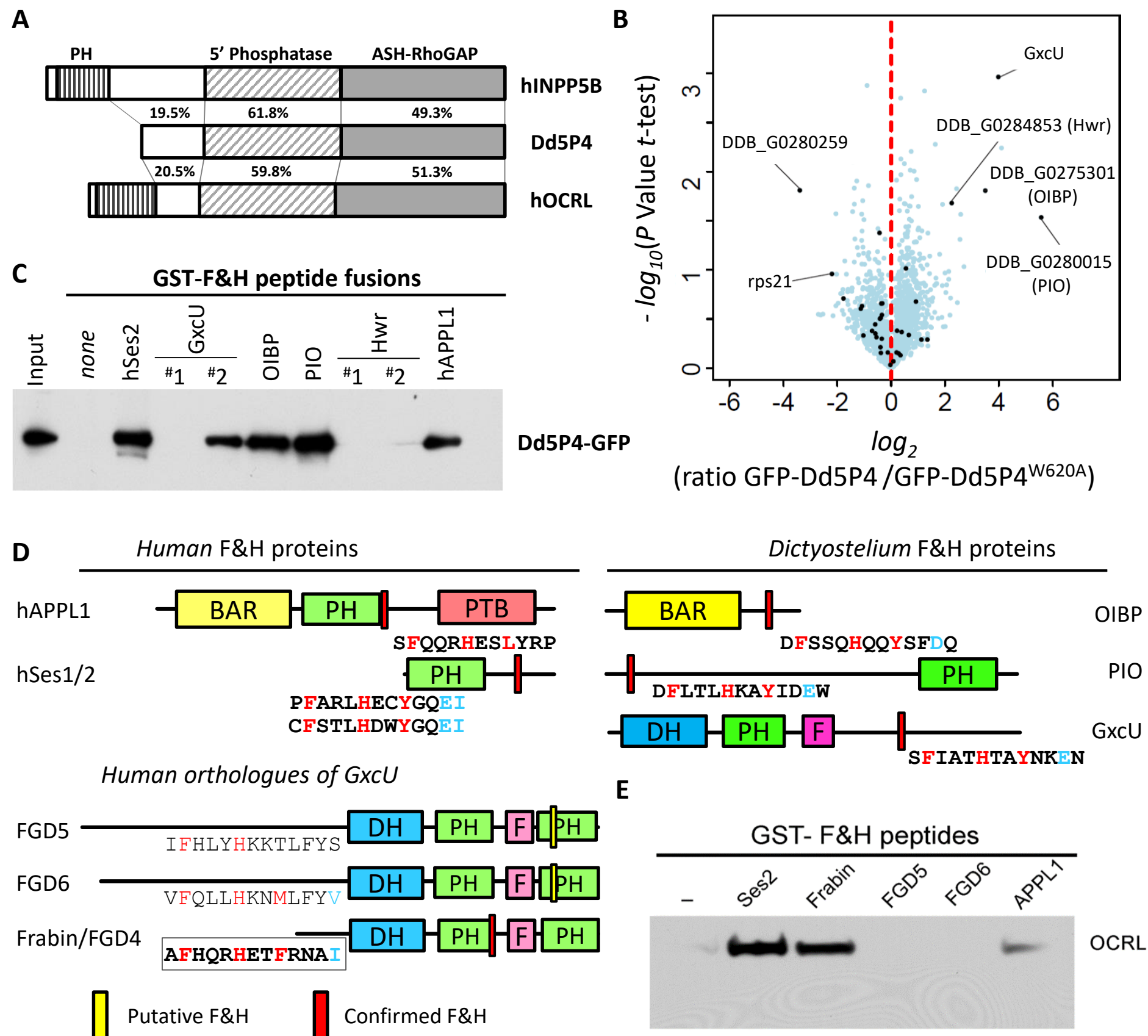
- 5 **Supplementary Movie 6, related to Figure 6:** 1:1 dilution-of imaging medium with distilled water
- 6 in *Dd5P4* mutants does not change CV exocytosis rate. Images 0.2 Hz. Scale Bar 15 μ m.

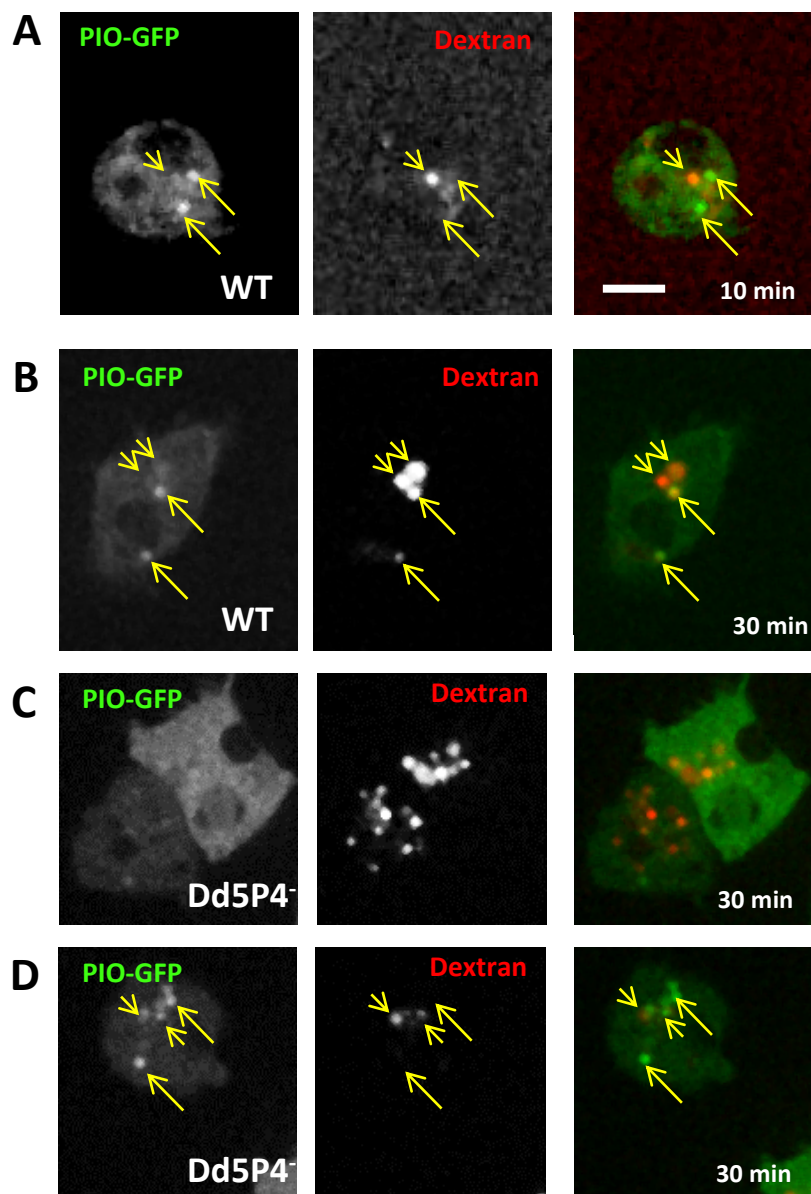
- 7 **Supplementary Movie 7, related to Figure 6:** the collapse/fusion phase of CV exocytosis in
- 8 *Dd5P4* mutants re-expressing GFP-Dd5P4. Images 0.2Hz. Scale Bar 15 μ m.

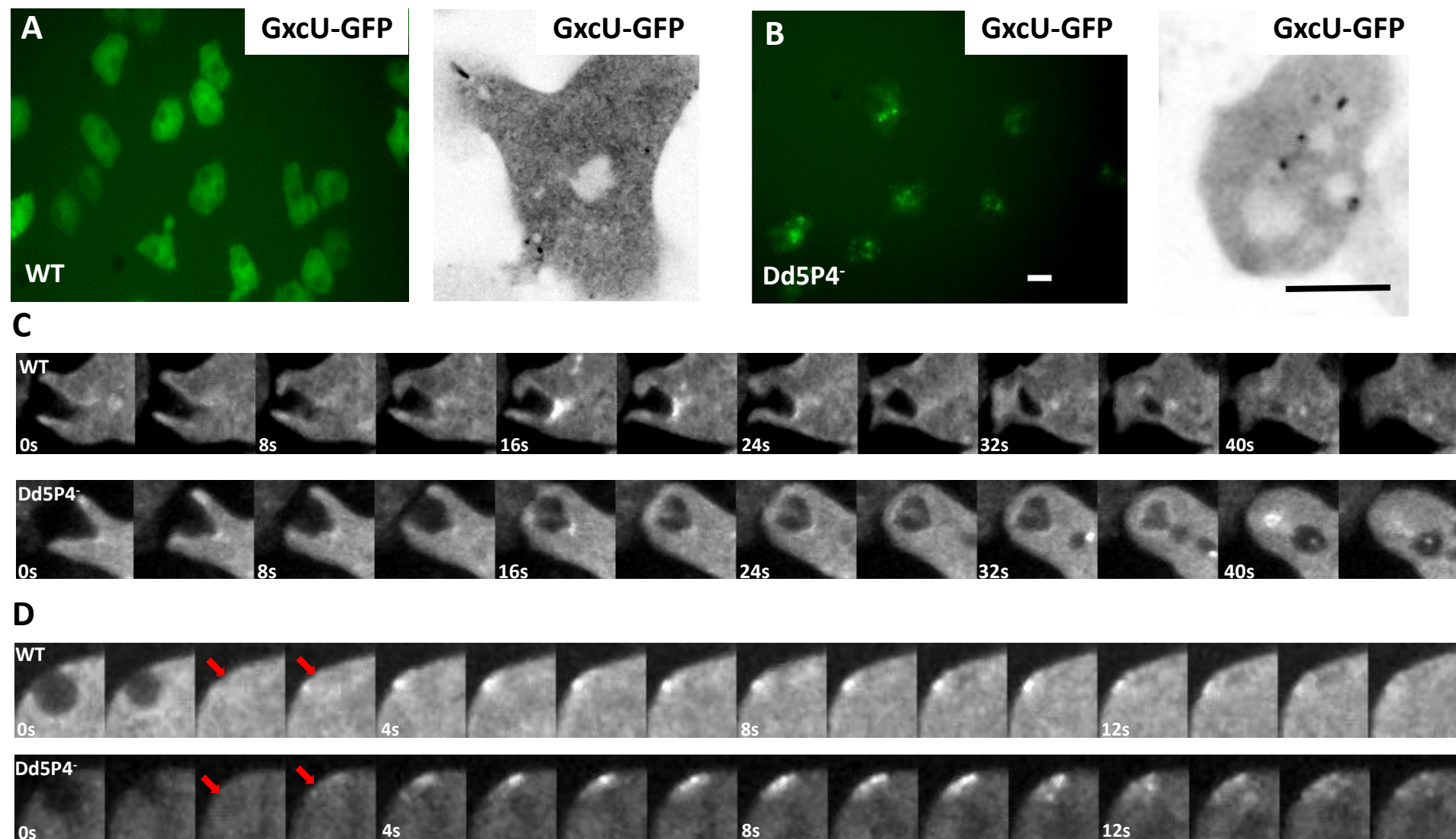
- 9 **Supplementary Movie 8, related to Figure 6:** the collapse/fusion phase of CV exocytosis in
- 10 *Dd5P4* mutants re-expressing F&H mutant GFP-Dd5P4^{W620A}. Images 0.2Hz. Scale Bar
- 11 15 μ m.

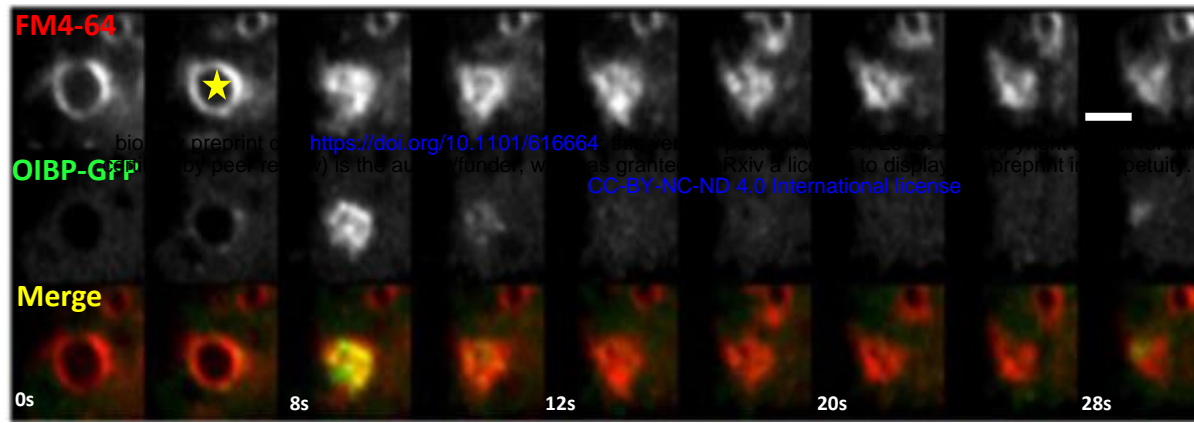
- 12



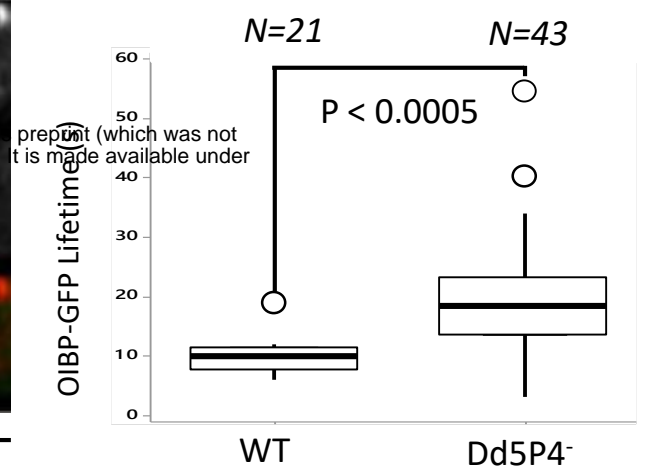




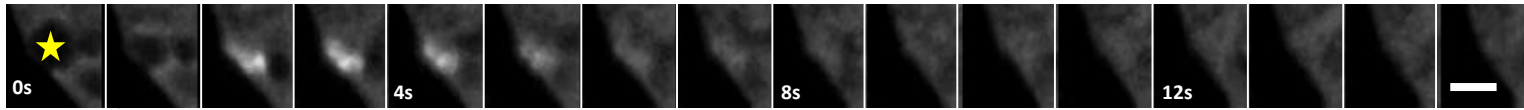


A

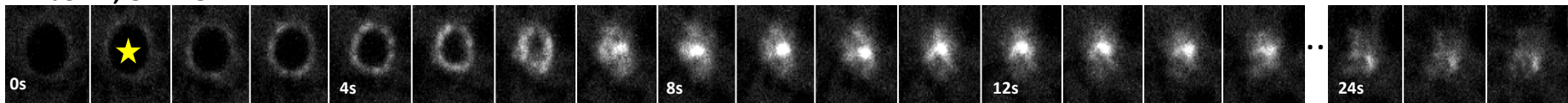
'Collapse phase'

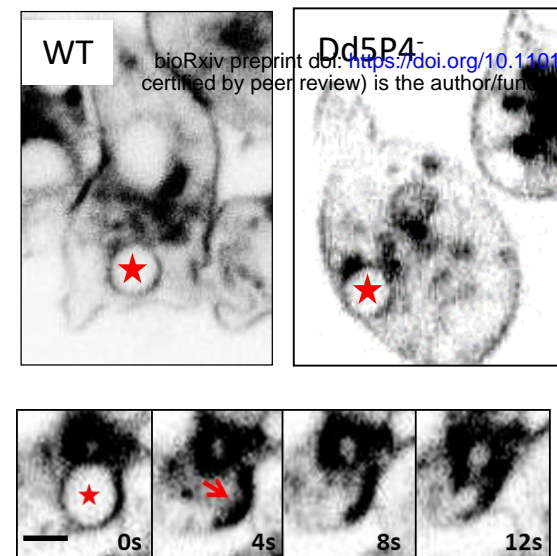
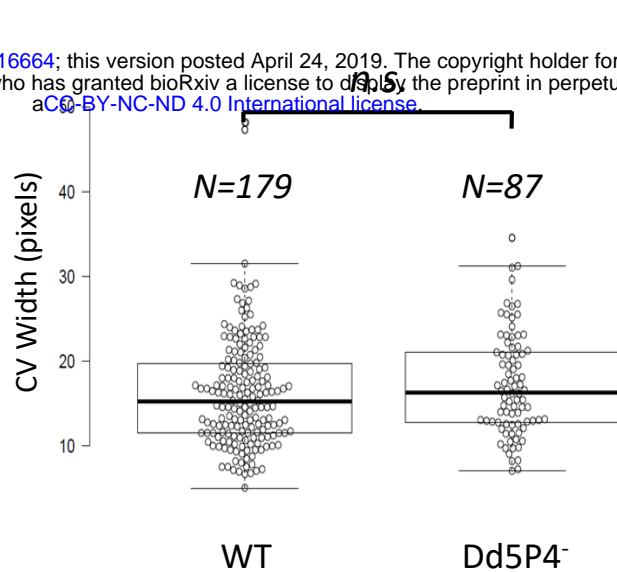
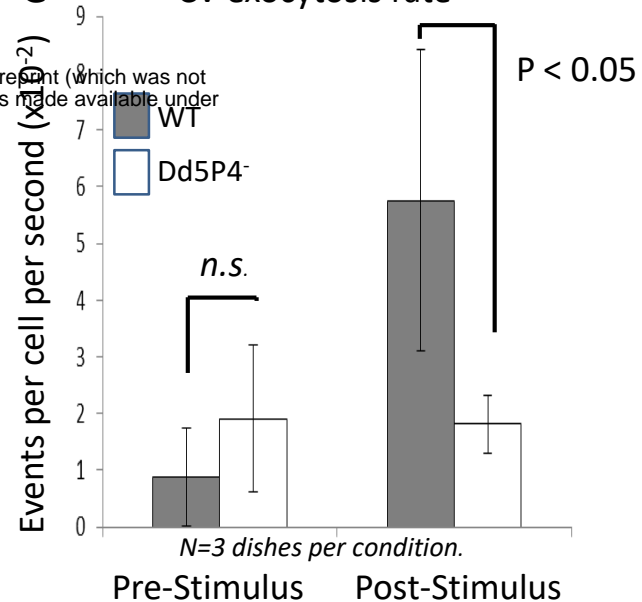
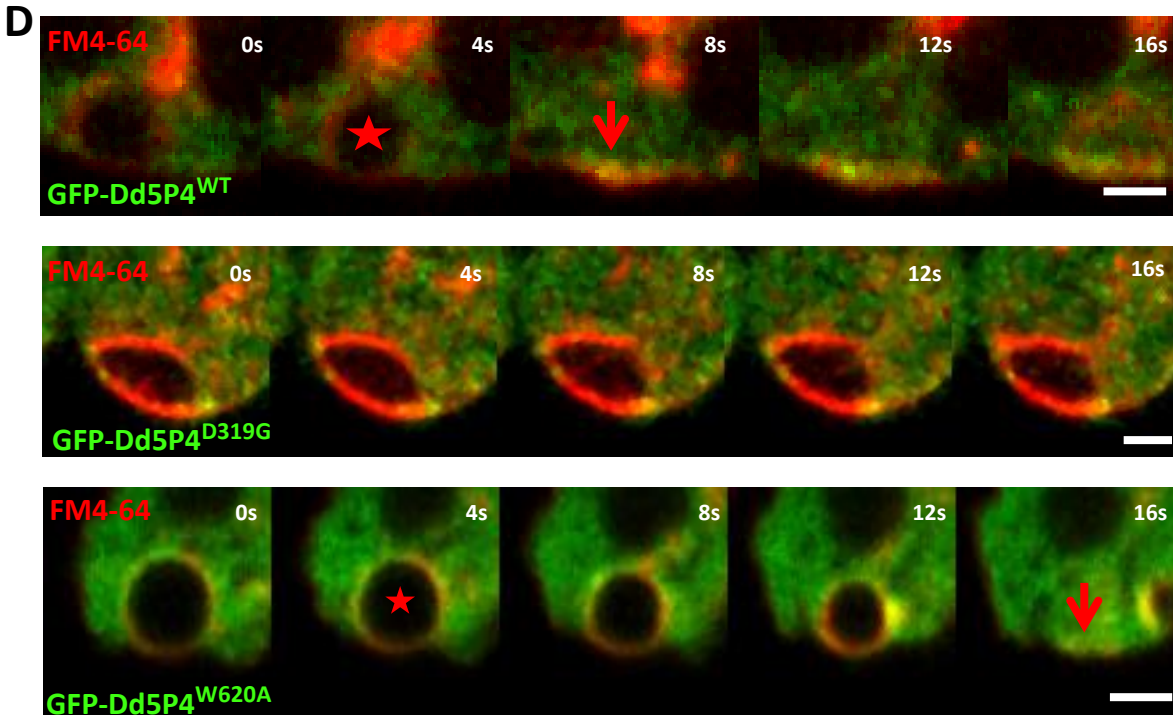
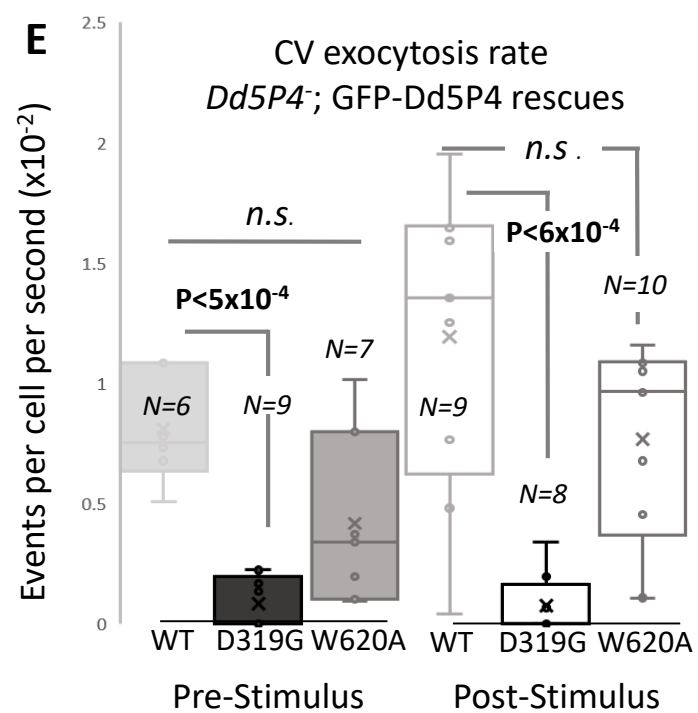
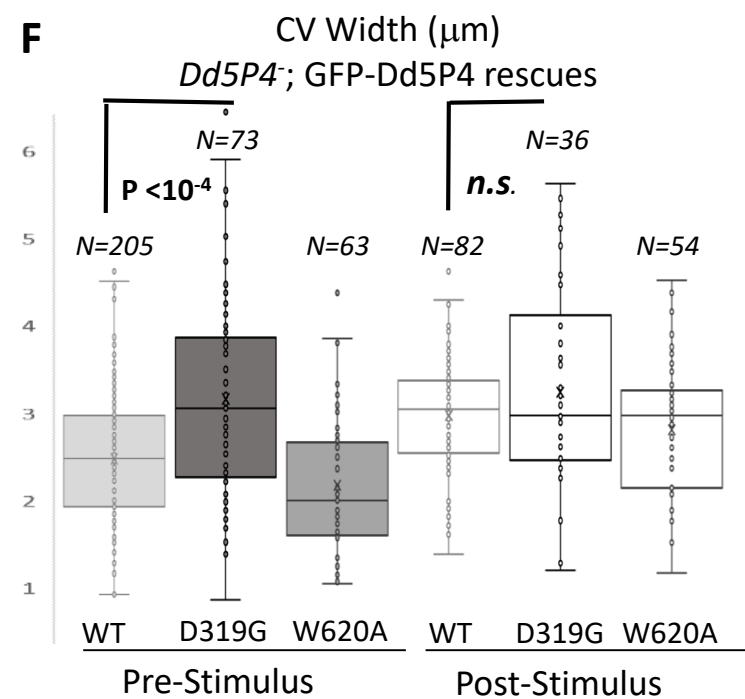
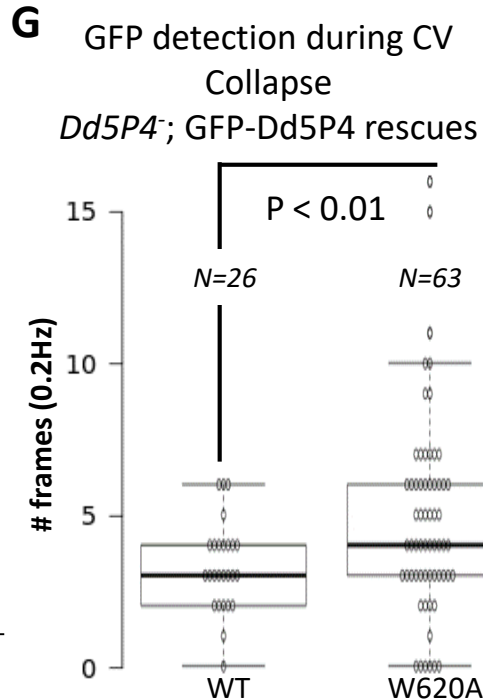
C**B**

WT; OIBP-GFP



Dd5P4⁻; OIBP-GFP



A**B** Fusion-competent CV Width (pixels)**C** CV exocytosis rate**D****E****F****G****H**

Model of Dd5P4 action during CV cycle

